

REPORT DOCUMENTATION PAGE

Form Approved
OMB No. 0704-0188

Public reporting burden for this collection of information is estimated to average 1 hour per response, including the time for reviewing instructions, searching existing data sources, gathering and maintaining the data needed, and completing and reviewing this collection of information. Send comments regarding this burden estimate or any other aspect of this collection of information, including suggestions for reducing this burden to Department of Defense, Washington Headquarters Services, Directorate for Information Operations and Reports (0704-0188), 1215 Jefferson Davis Highway, Suite 1204, Arlington, VA 22202-4302. Respondents should be aware that notwithstanding any other provision of law, no person shall be subject to any penalty for failing to comply with a collection of information if it does not display a currently valid OMB control number. **PLEASE DO NOT RETURN YOUR FORM TO THE ABOVE ADDRESS.**

1. REPORT DATE (DD-MM-YYYY) 17-08-2006		2. REPORT TYPE Journal Article		3. DATES COVERED (From - To)	
4. TITLE AND SUBTITLE Pentazole-Based Energetic Ionic Liquids: A Computational Study (Preprint)				5a. CONTRACT NUMBER	
				5b. GRANT NUMBER	
				5c. PROGRAM ELEMENT NUMBER	
6. AUTHOR(S) Ian S.O. Pimienta, Sherrie Elzey, Mark S. Gordon (Iowa State University); Jerry Boatz (AFRL/PRSP)				5d. PROJECT NUMBER 23030423	
				5e. TASK NUMBER	
				5f. WORK UNIT NUMBER	
7. PERFORMING ORGANIZATION NAME(S) AND ADDRESS(ES) Air Force Research Laboratory (AFMC) AFRL/PRSP 10 E. Saturn Blvd. Edwards AFB CA 93524-7680				8. PERFORMING ORGANIZATION REPORT NUMBER AFRL-PR-ED-JA-2006-300	
9. SPONSORING / MONITORING AGENCY NAME(S) AND ADDRESS(ES) Air Force Research Laboratory (AFMC) AFRL/PRS 5 Pollux Drive Edwards AFB CA 93524-70448				10. SPONSOR/MONITOR'S ACRONYM(S)	
				11. SPONSOR/MONITOR'S NUMBER(S) AFRL-PR-ED-JA-2006-300	
12. DISTRIBUTION / AVAILABILITY STATEMENT Approved for public release; distribution unlimited (AFRL-ERS-PAS-2006-222)					
13. SUPPLEMENTARY NOTES To be published in the Journal of Physical Chemistry					
14. ABSTRACT The structures of protonated pentazole cations (RN ₅ H ⁺), oxygen-containing anions such as N(NO ₂) ₂ ⁻ , NO ₃ ⁻ , and ClO ₄ ⁻ , and the corresponding ion pairs are investigated by <i>ab initio</i> quantum chemistry calculations. The stability of the pentazole cation is explored by examining the decomposition pathways of several monosubstituted cations (RN ₅ H ⁺) to yield N ₂ and the corresponding azidinium cation. The heats of formation of these cations, which are based on isodesmic (bond type conserving) reactions, are dependent on the nature of the substituents. The proton transfer reaction from the cation to the anion is investigated.					
15. SUBJECT TERMS					
16. SECURITY CLASSIFICATION OF:			17. LIMITATION OF ABSTRACT	18. NUMBER OF PAGES	19a. NAME OF RESPONSIBLE PERSON Dr. Scott Shackelford
a. REPORT	b. ABSTRACT	c. THIS PAGE			
Unclassified	Unclassified	Unclassified	A	61	19b. TELEPHONE NUMBER (include area code) N/A

Pentazole-Based Energetic Ionic Liquids: A Computational Study (PREPRINT)

Ian S.O. Pimienta¹, Sherrie Elzey¹, Jerry A. Boatz², and Mark S. Gordon¹

¹Department of Chemistry, Iowa State University, Ames, IA 50011

²Air Force Research Laboratory, Space and Missile Propulsion Division, AFRL/PRS, 10 E. Saturn Blvd., Edward AFB, CA 93524

Abstract:

The structures of protonated pentazole cations (RN_5H^+), oxygen-containing anions such as $\text{N}(\text{NO}_2)_2^-$, NO_3^- , and ClO_4^- , and the corresponding ion pairs are investigated by *ab initio* quantum chemistry calculations. The stability of the pentazole cation is explored by examining the decomposition pathways of several monosubstituted cations (RN_5H^+) to yield N_2 and the corresponding azidinium cation. The heats of formation of these cations, which are based on isodesmic (bond type conserving) reactions, are dependent on the nature of the substituents. The proton transfer reaction from the cation to the anion is investigated.

Introduction

There is growing interest in ionic liquids (ILs) as solvents for many applications including environmentally benign synthesis, catalysis, electrochemistry, and ion separation [1-5]. The chemical stabilities and very low vapor pressures of ILs make them suitable as alternatives to other more volatile organic solvents, hence the name “green” solvents [1-3]. By carefully selecting the starting cation and anion, the IL can be customized based on pre-selected characteristics (*e.g.* moisture stability, viscosity, density, miscibility), thus allowing the needed flexibility in the design of these materials.

Despite the “designer solvent” classification of stable ILs, it is important to remember [6,7] that they are not required to be stable. In fact a substantial number of ILs are chemically unstable, releasing large amounts of energy in the decomposition process. These so-called “energetic” ionic liquids may find some other useful applications [8]. The large positive heats of formation of cyclic nitrogen-rich cations make them promising precursors for the synthesis of highly energetic materials. One of the most widely studied IL cations is butyl-methyl-imidazolium (BMIM⁺). Molecular dynamics simulations of the IL BMIM⁺/PF₆⁻ indicate at least two different time scales for diffusion in such solvents and provide information on preferred structures [9,10]. The interaction of the surface layer of this IL with water has been studied experimentally [11] and the observed structural changes are consistent with the results of the computer simulations.

In order to increase the energy content (with the side effect of decreasing the stability) of the cation, BMIM⁺ may be replaced by the triazolium and tetrazolium cations, with three

and four nitrogens, respectively, in the ring. Recently, theoretical studies have been completed on ionic liquids based on the triazolium ($\text{N}_3\text{C}_2\text{H}_4^+$) and tetrazolium (N_4CH_3^+) cations, combined with anions such as dinitramide ($\text{N}(\text{NO}_2)_2^-$), nitrate (NO_3^-), and perchlorate (ClO_4^-) [12,13]. Another approach to increasing the energy of the cations is to introduce high-energy substituents into the ring, such as azido ($-\text{N}_3$) and nitro ($-\text{NO}_2$).

The present work is a systematic investigation of the structures and energetics of possible ionic liquids formed by protonated pentazole cations^{*}, RN_5H^+ , and the dinitramide, nitrate, and perchlorate anions.

There have been few attempts to synthesize HN_5H^+ as even its parent precursor, pentazole (HN_5), has proved to be difficult to isolate and detect. The first pentazole compounds to be synthesized were substituted by a phenyl ring [14-17]. Huisgen and Ugi prepared their phenyl-substituted pentazole by reacting the azide anion, N_3^- , with diazonium ions, ArN_2^+ , under careful temperature control [15,16]. The aryl pentazole products readily lost N_2 , but the resulting dimethylanilino pentazole was stable enough to allow an X-ray crystal structure determination. However, they were not successful in isolating HN_5 . Since then a significant goal of heterocyclic chemistry has been to prepare the parent pentazole. In earlier attempts, ozonolytic degradation of the aryl ring with a controlled amount of ozone was made but neither HN_5 nor its anion N_5^- was found [18]. Recently, Butler *et al.*, working under controlled conditions, were able to isolate and detect pentazole in solution as N_5^- with Zn^{2+} ion [19].

* The term pentazolium is not used since it refers to the deprotonated pentazole (N_5^+).

In addition to the experimental investigations, several theoretical studies have been performed on HN₅ as well [20-24]. Calculations predict that the half-life of HN₅ is only about 10 minutes [18]; this explains the difficulty in the direct detection of this compound. Chen [20] had initially suggested that HN₅ is a strong acid, even stronger than nitric acid; hence in solution a significant portion is easily converted to the anion, a fact finally corroborated by the experimental results of Butler *et al.* [19]. On the other hand, attempts to isolate the protonated pentazole cation have so far been unsuccessful and theoretical calculations are sparse [25,26]. The lack of experimental data on protonated pentazole makes accurate quantum chemical calculations essential in predicting the properties of these compounds.

The acidity of the azoles has been known for quite some time and increases in the order pyrrole < pyrazole < imidazole < 1,2,3-triazole < 1,2,4-triazole < tetrazole < pentazole [27]. This means that the protonated pentazole cation, which is the most acidic among the protonated azoles, is the most difficult to isolate experimentally. Mo *et al.* investigated [26] the basis set effects on the theoretical (Hartree-Fock) gas-phase basicities of several azoles including pentazole and its protonated form with the STO-3G, 3-21G, and 6-31G basis sets, using the conjugate gradient optimization procedure [28] to obtain the starting structures. The basicity of these compounds is predicted to depend on the contributions of different tautomers of either the nonprotonated or protonated forms.

The monosubstituted pentazole cation has three possible isomers, i.e., 1-H,3-R-1,3-pentazole (I), 1-H,2-R-1,2-pentazole (II), and 1-H,1-R-1,1-pentazole (III) ions (see Figure 1). The only difference among the three isomers is in the location of the substituent R. In order to find new high-energy IL precursors and obtain a more comprehensive picture of the stability of these compounds, several topics will be addressed below. First, the stability and structure of several monosubstituted pentazole cations are investigated by determining the activation barrier and the energy of decomposition to N_2 and the corresponding azidinium cation. It is expected that substituents may play a major role in the thermodynamic stability of the protonated pentazole ring. Second, π bonding and population analysis are performed to determine the amount of charge delocalization around the ring in these compounds. One of the characteristics of low melting ILs is the presence of charge-delocalized ions. Finally, the structures of dimers composed of the protonated pentazole and several energetic anions including dinitramide, nitrate, and perchlorate are presented. All possible structures including the neutral pairs, transition states, and ionic pairs are described. The small barriers for proton transfer from the cation to the anion indicate that deprotonation may be a first step in the decomposition of these pentazole-based ILs.

Computational Details

The geometries of the monosubstituted pentazole cations RN_5H^+ ($R \equiv H, F, CH_3, CN, NH_2, OH, OCH_3, CH_2NO_2, C_2H_5, N_3, NF_2$), transition state structures, and decomposition products as well as the anions dinitramide, nitrate, and perchlorate were fully optimized with second order Møller-Plesset perturbation theory (MP2), [29,30] using the restricted

Hartree-Fock (RHF) [31] determinant as the reference. The CR-CCSD(T) (completely renormalized coupled-cluster with singles, doubles, and noniterative triples) [32-34] method was used to calculate single point energies for the cations at the MP2 geometries. The basis set used was 6-311++G(d,p) [35,36] for all calculations. Intrinsic reaction coordinate (IRC) calculations were performed to connect the transition states with the reactants and products [37]. An MCSCF [38] calculation using Edmiston-Ruedenberg molecular orbitals (LMO) [39] was performed to determine the amount of charge delocalization in the ring [12,13]. Gaussian-2 (G2) [40,41] calculations were employed to extract data for the thermochemical analysis. Ion pairs of several neutral, transition state, and ionic dimers were optimized at the RHF level, and MP2 single point energies at the RHF geometries were calculated. All results were obtained from the GAMESS [42,43] electronic structure package, except for the G2 results, which were obtained from the Gaussian94 code [44]. All molecules were visualized with MacMolPlt [45].

Results and Discussion

Minimum Energy Structures

The MP2/6-311++G(d,p) optimized structures for the anions and their protonated counterparts that are used to construct the dimer structures are shown in Figure 2. There is very little change in the geometries between the protonated and deprotonated structures of the nitrate and perchlorate species. However, the dinitramide anion has protonation sites at both the central nitrogen and any of the four oxygens; only the structure with the preferred site of protonation, i.e. the central nitrogen, is shown.

The optimized geometries for the monosubstituted pentazole cations I (Figure 3) and II (Figure 4) are summarized in Tables 1 and 2, respectively. MP2/6-311++G(d,p) geometry optimizations of the 1,1-pentazole cations III lead to the instantaneous decomposition to N_2 and the corresponding azidinium cations, as illustrated in Figure 5 for $R \equiv H$ -, F -, CH_3 -, CN -, NF_2 -, and CH_2NO_2 . For $R \equiv NH_2$ -, OH -, OCH_3 -, the azidinium cations break down further, ejecting another N_2 . For $R \equiv C_2H_5$ -, the 1,1-pentazole cation decomposes into two N_2 molecules, with cyclization of the remaining $NHC_2H_5^+$ species. It is interesting to see in Figure 5 that the N_3 -substituted cation spontaneously decomposes into pieces, forming N_2 molecules and H^+ .

Like their neutral parent HN_5 [24], the cationic pentazole rings in all monosubstituted species for isomers I and II are planar, with almost equal N–N bond lengths of ~ 1.32 Å (Tables 1, 2). The maximum difference in N–N bond distances is only 0.038 Å in isomer I for $R \equiv CN$ -, with the N_3 – N_4 and N_1 – N_5 bonds always slightly longer than the other N–N bonds in the ring (see Figure 1 for the atom numbering). This difference is slightly smaller in isomer II (about 0.027 Å for $R \equiv F$) where, in general, the N_3 – N_4 bond is a little longer than the remaining N–N bonds. These results indicate that the cationic pentazole ring is hardly affected by the attached substituents regardless of how small ($-H$) or bulky ($-NF_2$) the groups are, and the strength of their electron-donating ($-OH$ and $-NH_2$) or electron-withdrawing ($-CN$) character. The very small variation in the NN distances also suggests significant electron delocalization.

MP2 geometry optimization of the nitro group (-NO₂) results in a rather long N–N distance of 2.684 Å, suggesting very weak binding to the ring nitrogen. This is not surprising, since it was shown previously that -NO₂ does not bind well to a nitrogen of the tetrazolium ring [10]. In the present work, a methylene spacer, -CH₂NO₂, is inserted to facilitate binding.

Relative Energies of Monosubstituted Pentazole Cations

The two stable ring isomers of the monosubstituted pentazole cations (labeled I and II in Figure 1) have two possible resonance structures, shown in Figure 6, that differ in the positions of the double bonds and the location of the cationic charge. The molecular and electronic structure of each isomer is some composite of these contributing resonance structures, i.e. IA and IB for isomer I and IIA and IIB for isomer II. For all substituted species, MP2/6-311++G(d,p) predicts that isomer I is lower in energy than isomer II by ~16 – 22 kcal/mol (see Table 3). For comparison, the CR-CCSD(T) single point energies at the MP2 geometries predict that isomer I is lower by ~15 – 21 kcal/mol.

The transition state for proton rearrangement in the hydrogen-substituted cations (HN₅H⁺), from the 1-H,2-H-N₅⁺ species to its more stable 1-H,3-H-N₅⁺ counterpart, lies 50 kcal/mol above the less stable isomer (see Figure 7). This means that it is rather unlikely for proton migration to occur, although chemical intuition suggests that steric effects due to bulky substituents attached to N2 in the pentazole ring, such as -CH₂NO₂ and -NF₂, may lower this barrier.

In order to assess the relative importance of the contributing resonance structures with regard to the amount of charge delocalization around the pentazole ring in the parent isomers, an MCSCF π LMO population and π bond order analysis [12,13] has been performed. Recall that the possibility of obtaining a low melting point IL is enhanced by substantial charge delocalization around the protonated pentazole ring. The diagonal elements of the density matrix can be regarded as the number of electrons occupying the LMO, while the off-diagonal elements give the π bond orders. A positive bond order reflects a bonding interaction and a negative bond order indicates an antibonding interaction. The strength of these interactions is measured by the magnitude of their respective bond orders.

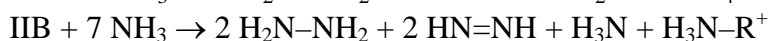
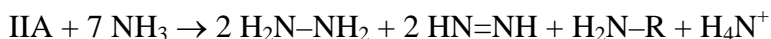
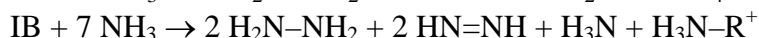
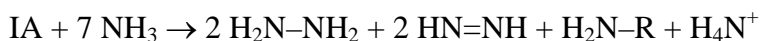
The results of the MCSCF bonding analysis for the parent pentazole cations are presented in Table 4. For the resonance structures of isomer I, if IA dominated over IB, N1 would have two π electrons and all other atoms in the ring would possess one π electron (see Figure 6). Table 4 shows that N1 and N3 have π populations of 1.37 and 1.39 electrons, respectively, indicating nearly equal contributions from the two resonance structures. So, these two nitrogens equally share the formal charge of +1 in isomers IA and IB. For isomer II, both N1 and N2 have the same population of 1.42 π electrons, which means that the ring is a hybrid between IIA and IIB and that the resonance structures are of equal importance. These observations are further validated by the calculated π bond orders of 0.50 – 0.70 between adjacent atoms. These bond orders between 0 and 1 also suggest that the ring is delocalized. For both isomers, all next nearest neighbor interactions are antibonding. The calculated total π bonding of 1.89, obtained by

summing all π bonding and all π antibonding interactions, is very close to the total bonding of 2 π bonds in diagrams IA, IB, IIA, and IIB shown in Figure 6.

Heats of Formation

The amount of energy contained in the monosubstituted pentazole cations may be quantified via their heats of formation, calculated here by combining their MP2/6-311++G(d,p) electronic energies with the data obtained from the G2 calculations. It is expected that the pentazole cation, in which all the atoms in the ring are nitrogens, will have a larger heat of formation than tetrazolium or triazolium.

The calculated gas-phase heats of formation for both monosubstituted pentazole cations are presented in Table 5. In order to obtain accurate heats of formation for these cations, several isodesmic (bond type conserving) reactions are utilized. Since there are two contributing resonance structures each for both isomers, four isodesmic reactions are considered (two for isomer I, i.e. IA and IB, and two for isomer II, i.e. IIA and IIB):



Because isodesmic reactions conserve the number of formal bond types on both sides of a reaction, the correlation energy [46] error is minimized and, hence, the computed enthalpies of formation are more accurate due to error cancellations. Table 5 shows that the calculated heats of formation for IA and IB (or IIA and IIB) are almost always equal, with the largest deviation of only 3.3 kcal/mol obtained from the NF_2 -substituted ion.

Thus, the average values of IA and IB and of IIA and IIB can be regarded as the heats of formation for the monosubstituted pentazole cations I and II, respectively.

As expected, the average heats of formation for the monosubstituted pentazole cations are huge, about 286.8 kcal/mol for the parent H-substituted pentazole cations. In comparison, the predicted heats of formation for the parent triazolium and tetrazolium cations are 196.5 [12] and 254.1 [13] kcal/mol, respectively. This is further evidence that these pentazole ions are relatively unstable and, therefore, will likely be difficult to synthesize, isolate, and detect, much like their parent neutral pentazole. The heats of formation of the monosubstituted pentazole cations I are always smaller by about 15.5—20.6 kcal/mol relative to cations II.

Of course, the nature of the substituent attached to the pentazole ring affects the computed enthalpy of formation. By replacing the -H substituent in the parent pentazole cation by electron-donating groups (EDGs), the calculated heats of formation decrease, while electron-withdrawing groups (EWGs) tend to increase the enthalpies. For the monosubstituted isomer I, the heats of formation, in kcal/mol, are decreased by the presence of EDGs by as little as 2.8 (-OH) to as much as 17.6 (-CH₃), and increased by EWGs by as little as 22.0 (-F) to as much as 106.8 (-N₃) relative to the enthalpy for the parent H-substituted 1,3-pentazole ion (285.6 kcal/mol). These differences in enthalpies are 3.7, 19.4, 24.2, and 104.0 kcal/mol for the -OH, -CH₃, -F, and -N₃ substituents, respectively, relative to the parent 1,2-pentazole ion (303.9 kcal/mol). However, the cations with nitrogen-containing EDGs such as -NH₂ and -NF₂ have higher heats of

formation, in opposition to the main trend. In these instances, the resulting increase in the calculated enthalpy is due to the additional nitrogen adjacent to the pentazole ring. All listed heats of formation in Table 5 are large and positive, but the species with the largest enthalpies on a per weight basis include the parent pentazole cations with heats of formation of about 4.1 kcal/g and the CN-substituted ions with energies of about 3.8 kcal/g.

Transition States and Decomposition Products

The transition state structures for the decomposition of the monosubstituted cations I, $\text{RN}_5\text{H}^+ \rightarrow \text{RN}_3\text{H}^+ + \text{N}_2$, (Figure 8) show a lengthening of the N1–N5 and N3–N4 bonds by about 0.2 – 0.5 Å and shortening of the N4–N5 distance by about 0.13 Å (see Figure 1 and Table 6), in the process of eliminating an N_2 molecule. In general, the N3–N4 bond length is longer than the N1–N5 distance, implying that the transition state is obtained via an asymmetric ring opening. The exception is the parent 1,3-pentazole ion (i.e. the H-substituted) formed through a symmetric ring opening mechanism with equal N3–N4 and N1–N5 bond lengths. The decomposition of the monosubstituted cations II, on the other hand, involves two steps. First, the N2–N3 distance increases by ~ 0.5 – 0.7 Å, while the N3–N4 bond decreases by ~ 0.17 Å forming ring-opened transition states (see Figure 9 and Table 7), leading to the local minimum structures shown in Figure 10 and quantified in Table 8. There is a slight increase in the N4–N5 bond length of about 0.05 Å, which indicates that a succeeding step to form N_2 is imminent. Indeed, the second step involves the formation of transition states (Figure 11) in which the N4–N5 distance is increased further by about 0.6 Å (Table 9). It is interesting to note from the structures in Figure 11

that the hydrogen in the azidinium cation located in the N1 position is oriented in such a way that it may be involved in a rearrangement reaction into the more stable form in which the hydrogen is farthest away from the substituents. The one exception to this is the CH_2NO_2 -substituted cation in which the hydrogen in the N1 position is transferred to one of the oxygens in the CH_2NO_2 moiety.

The structures of the decomposition products of the various monosubstituted pentazole cations for both isomers are shown in Figures 12 and 13. The optimized geometries for the products are listed in Tables 10 and 11. The decomposition of the monosubstituted pentazole cations involves the formation of N_2 . The resulting bond distance of 1.12 Å in the product NN bonds for all isomer I and II decomposition products is in good agreement with the experimental value of 1.098 Å. Figure 13 confirms that the hydrogen in the azidinium cation, originally located in the N1 position, migrates to form the more stable isomer, similar to that of the isomer I decomposition products. As noted above, the exception is the CH_2NO_2 -substituted azidinium ion, in which the hydrogen is transferred to the oxygen in the nitro group instead, producing three decomposition products; N_2 , HONO, and H_2CN_3^+ .

The activation energies for the decomposition reactions are listed in Table 12. Isomer I decomposes in a single step via an asymmetrically ring-opened transition state (see Figure 8 and Table 6), while isomer II decomposes in two steps via a ring opening followed by a subsequent proton migration (Figures 9 and 11 and Tables 7 and 9). All of the monosubstituted isomer I species have CR-CCSD(T) activation energies in the 20 –

30 kcal/mol range. The CR-CCSD(T) E_{a1} activation energies of isomer II are larger by $\sim 2 - 7$ kcal/mol, except for $R \equiv F, CN,$ and NF_2 . Previous studies on several neutral azoles, including triazole, tetrazole, and pentazole, show that the activation energies for this family of azoles depend on the number of ring nitrogen atoms and increase in the order pentazole < tetrazole < triazole [24]. It is expected that their monosubstituted cationic counterparts will follow the same trend.

Table 12 shows that EDGs in isomer I such as $-CH_3,$ $-CH_2NO_2,$ and $-C_2H_3$ tend to give the largest activation energies (24.0, 22.6. and 21.8 kcal/mol, respectively) while EWGs such as $-N_3$ (16.0 kcal/mol) and $-CN$ (19.0 kcal/mol) give the smallest barriers. The E_{a1} activation energies are slightly larger in isomer II, but the observed trend is the same. Isomer II with EDGs attached, *e.g.* $-CH_3$ (37.0 kcal/mol) and $-C_2H_3$ (32.0 kcal/mol), possess larger activation energies than their EWG-substituted counterparts such as $-N_3$ (23.4 kcal/mol) and $-CN$ (19.0 kcal/mol). In general, the CR-CCSD(T) activation barriers are at most 5 kcal/mol larger than the MP2 activation energies. The inductive effects (*e.g.* in $-CH_3$ and $-CH_2NO_2$) and resonance donating effects (*e.g.* in $-C_2H_3$) brought about by the EDGs help to stabilize the ring by increasing the electron density in the ring, thereby resulting in higher activation energies. Although isomer I is lower in energy, isomer II is more stable to decomposition.

An important factor in the design of high-energy materials is the energy released on decomposition. The performance of a highly energetic system is greatly enhanced with an increase in the released energy. The decomposition reactions for all monosubstituted

species are exothermic (see Table 13). In general, the decomposition of isomer II is more exothermic by at least 14 kcal/mol relative to isomer I. As for the activation energy, the decomposition energy is greatly affected by the substituent attached in the cationic pentazole rings of the two isomers. The decomposition becomes more exothermic with an increase in the electron-withdrawing character of the substituent. The highest decomposition energies are found in the NH_2 - and N_3 -substituted cations for isomer I (-24.5 and -24.0 kcal/mol, respectively) and the N_3 - and CH_2NO_2 -substituted cations for isomer II (-58.9 and -56.1 kcal/mol, respectively). The observed trend, in which a more exothermic reaction is accompanied by a lower activation barrier, seems to follow Hammond's postulate [47], according to which a lower activation energy corresponds to a more exothermic reaction. By combining the energy profiles for the decomposition of the monosubstituted pentazole cations including the minimum energies, the activation energies, and the energies for decomposition, a general potential energy pathway for decomposition can be deduced for isomers I and II (Figure 14). Finally, note that there are several cases in both Tables 12 and 13 for which there is significant (>10 kcal/mol) disagreement between the MP2 and CR-CCSD(T) energy differences. For example, the two levels of theory differ by ~ 14 kcal/mol in their prediction of the net reaction energy for the parent species (Table 13), with $\text{R}=\text{H}$. Such disagreement is often indicative of some non-trivial configurational mixing, in which case the coupled cluster method is generally more reliable.

Ion Pair Interactions

The RHF/6-311++G(d,p) optimized structures of the neutral and ionic pairs, as well as the transition states that connect them, for all dimers formed by combining either of the H-substituted cationic pentazole isomers with the three selected anions are shown in Figures 15-23. All MP2/6-311++G(d,p) optimizations and structure determinations were unsuccessful in locating ionic dimers; only hydrogen-bonded neutral pairs seem to exist. However, MP2 single point energies at the RHF geometries, referred to as MP2//RHF, are calculated for comparison.

The results of the RHF/6-311++G(d,p) geometry optimizations on several different orientations of either of the two minimum energy protonated pentazole isomers and the minimum energy dinitramide anion indicate that the dimer structure in Figure 15, brought about by the transfer of the proton from the 1,2-isomer to the dinitramide, is the most stable neutral dimer. Henceforth, this structure is taken as the zero energy structure against which all other energies of the remaining protonated pentazole-dinitramide dimer structures are compared. However, the neutral dimer structure formed by the protonated 1,3-pentazole and dinitramide is higher in energy by only 0.4 and 1.0 kcal/mol at the RHF and MP2 levels of theory, respectively. The MP2//RHF energy is taken to be the MP2 zero of energy.

In the search for the minimum energy protonated pentazole-dinitramide dimer structures, several RHF optimizations were performed. The starting structures were varied with an adequate cation-anion separation to remove any biases towards the final optimized structures. Figures 16, 18, 19, and 21 show that only a few neutral and ionic dimer pairs,

out of about 20 starting structures, were found, depending on the location of the protonation in dinitramide. In particular, the number of unique protonated pentazole-dinitramide ionic dimer structures is only four for isomer I (Figure 16) and three for isomer II (Figure 19). The small number of dimer structures found is due to the highly symmetric character of the starting protonated pentazole and the fact that the cationic pentazole ring is composed of all nitrogens, which means that some of the initial dimer orientations converge to the same final structure.

The corresponding neutral dimer structures resulting from proton transfer reactions from the cation to the anion are shown in Figures 18 and 21. The transition states linking the ionic pairs to the neutral dimers are shown in Figures 17 and 20. As noted previously, (Figure 16), the common zero of energy for all structures is the most stable pentazole-dinitramide neutral dimer, shown here as the leftmost structure in Figure 21. The calculated MP2 activation energies show shallow barriers for proton transfer with the highest value only ~4.5 kcal/mol. This is indicative of the very short lifetimes of these ionic pairs, if they were synthesized. In fact, only two of the ionic dimers have a barrier; in almost all cases the proton is spontaneously transferred to the dinitramide anion to form the neutral pairs.

The calculated energies for the neutral dimer structures in Figures 18 and 21 show that the preferred protonation site in the dinitramide anion is indeed the central nitrogen. For all seven neutral structures of the pentazole-dinitramide pairs, the energy separation is small with a maximum difference at the RHF and MP2 levels of only 11.9 and 14.0

kcal/mol, respectively. The structures in Figures 18 and 21 show that the predominant form of interaction is intermolecular hydrogen bonding, either the N–H---N or O–H---N type, but a few dimer structures possess intramolecular hydrogen bonding within the dinitramic acid moiety such as the O–H---O bonding interaction found in Figure 18(d).

The interactions between each of the protonated pentazole isomers with the nitrate and the perchlorate anions were also examined. The MP2 optimizations result in an instantaneous proton transfer from the protonated pentazole to one of the oxygens of the anion, whereas RHF optimizations predict that both neutral and ionic dimers are local minima. So, electron correlation is clearly important in determining which structures exist. Figures 22 and 23 show the neutral and ionic dimer structures and the transition states that connect them. The pair comprising the H-substituted 1,2-pentazole and either the nitrate or perchlorate anion is predicted to be lower in energy than the interaction between the H-substituted 1,3-pentazole and these anions. The zero energy structure for the neutral pentazole-nitrate pair, resulting from the transfer of a proton from isomer II to the nitrate, is shown in the bottom rightmost corner of Figure 22. The lowest energy protonated 1,3-pentazole-nitrate pair obtained in the MP2 (RHF) calculation is only 1.7 kcal/mol (1.3 kcal/mol) higher in energy relative to this structure. In the protonated pentazole-perchlorate pair, the MP2 energy separation between the two neutral dimer structures is 2.1 kcal/mol.

Finally, the MP2 heats of reaction for the formation of either the neutral or ionic dimers from the individual ions are included as the third number in Figures 16, 18, 19, 21, 22,

and 23. The mixing of the protonated pentazole with any of the three anions produces either neutral or ionic pairs, although MP2 optimizations result in proton transfer. These reactions are all highly exothermic. As expected, the heats of reaction for the formation of the neutral pairs are always larger (more exothermic) than those for the ionic pairs, by at least 16 kcal/mol in the protonated pentazole-dinitramide, 31 kcal/mol in the protonated pentazole-nitrate, and 20 kcal/mol in the protonated pentazole-perchlorate systems. The neutral dimer containing 1,3-pentazole is lower in energy than the corresponding 1,2-isomer by only 1.2, 1.7, 2.2 kcal/mol for the dinitramide, nitrate, and perchlorate anions, respectively. The differences in the heats of reaction between the ionic dimers of the two isomers are at least 2.0, 3.5, and 6.5 kcal/mol, respectively, for the dinitramide, nitrate, and perchlorate anions. Although the parent isomer I is more stable than isomer II, the anions seem to prefer to bind to the latter.

Conclusions

Ionic liquid dimers composed of the five-membered monosubstituted pentazole cation and the dinitramide, nitrate, and perchlorate anions have been investigated. Of the two monosubstituted pentazole cation isomers, it is predicted that the 1,3-isomer is lower in energy than the 1,2-isomer. The relative activation energies and decomposition energies for the decomposition of these cations to N_2 + the corresponding azidinium cation can be related to the electron-donating character of the substituent. An electron-donating substituent tends to increase the activation energy and decrease the decomposition energy. The MCSCF π orbital analysis suggests that the electrons in the cationic pentazole ring are delocalized. The calculated enthalpies of formation show that electron-

withdrawing groups such as -CN and -N₃ help to increase the heats of reaction. Several dimer structures composed of the H-substituted pentazole and either of the anions mentioned above are proposed and found to be very unstable. The low barrier connecting the ionic and neutral dimers, and the large corresponding exothermicity suggests that a proton is spontaneously transferred to the anion. So, a fundamental step for the decomposition of protonated pentazole is likely to be deprotonation. However, the introduction of additional ion pairs are likely to stabilize the charge separation in the ionic species.

The CR-CCSD(T) activation energies for decomposition of the 1,2- and 1,3- cations are in the range of 22-31 and 20-28 kcal/mol, respectively. Since a higher barrier corresponds to a more stable species, the most desirable substituents from this perspective are H, CH₃, CH₂NO₂, and C₂H₃ for both isomers, and OCH₃ as well for the 1,2-isomer. Since all of the substituted species are highly exothermic, the stability to decomposition should be the overriding factor.

Acknowledgements

This work was supported in part by grants from the Air Force Office of Scientific Research and the National Science Foundation. The authors thank Dr. Michael Berman for suggesting this study and Dr. Michael W. Schmidt and Dclt. Deborah D. Zorn for their helpful discussions. The computations were performed on local computers, including an AXP cluster paid for in part by a DoD DURIP equipment grant, and an IBM

cluster provided by two Shared University Research grants from IBM, augmented by funds from the US Departments of Defense and Energy.

References

- (1) *Ionic Liquids, Industrial Applications to Green Chemistry*, ACS Symposium Series 818, R. D. Rogers, K. R. Sheldon, Eds. (2002).
- (2) Welton, T. *Chem. Rev.* **99**, 2071-2083(1999).
- (3) Larson, A. S., Holbrey, J. D., Tham, F. S., Reed, C. A. *J. Am. Chem. Soc.* **122**, 7265-7272(2002).
- (4) Sheldon, R. *Chem. Commun.* 2399-2407(2001).
- (5) Wasserscheid, P., Keim, W. *Angew. Chem., Int. Ed. Engl.* **39**, 3772-3789(2000).
- (6) Wilkes, J. S. *Ionic Liquids, Industrial Applications to Green Chemistry*, ACS Symposium Series 818, R. D. Rogers, K. R. Sheldon, Eds. (2002), pp 214-229.
- (7) Wilkes, J. S. *Green Chem.* **4**, 73-80(2002).
- (8) Drake, G., Hawkins, T., Brand, A., Hall, L., McKay, M., Vij, A., Ismail, I. *Propellants, Explosives, Pyrotechnics* **28**, 174-180(2003).
- (9) Margulis, C. J., Stern, H. A., Berne, B. J. *J. Phys. Chem. B* **106**, 12017-12021 (2002).
- (10) Morrow, T. I., Maginn, E. J. *J. Phys. Chem. B* **106**, 12807-12813(2002).
- (11) Rivera-Rubero, S., Baldelli, S. *J. Am. Chem. Soc.* **126**, 11788-11789(2004).
- (12) Schmidt, M. W., Gordon, M. S., Boatz, J. A. *J. Phys. Chem. A* **109**, 7285-7295 (2005).
- (13) Zorn, D. D., Boatz, J. A., Gordon, M. S. submitted.
- (14) Clausius, K., Hürzeler, H. *Helv. Chim. Acta* **37**, 798(1954).
- (15) Huisgen, R., Ugi, I. *Angew. Chem.* **68**, 705-706(1956).
- (16) Huisgen, R., Ugi, I. *Chem. Ber.* **90**, 2914-2927(1957).
- (17) Ugi, I. *Angew. Chem.* **73**, 172(1961).
- (18) Benin, V., Kaszynski, P., Radziszewski, J. G. *J. Org. Chem.* **67**, 1354-1358 (2002).
- (19) Butler, R. N., Stephens, J. C., Burke, L. A. *Chem. Commun.* **8**, 1016-1017(2003).
- (20) Chen, C. *Int. J. Quantum Chem.* **80**, 27-37(2000).
- (21) Ferris, K. F., Bartlett, R. J. *J. Am. Chem. Soc.* **114**, 8302-8303(1992).
- (22) Inagaki, S., Goko, N. *J. Am. Chem. Soc.* **109**, 3234-3240(1987).
- (23) Catalan, J., de Paz, J. L. G., Yanez, M., Elguero, J. *Chem. Scripta* **24**, 84-91 (1984).
- (24) Hammerl, A., Klapötke, T. M., Schwerdtfeger, P. *Chem. Eur. J.* **9**, 5511-5519 (2003).
- (25) Belau, L., Haas, Y., Zilberg, S. private communications.
- (26) Mó, O., de Paz, J. L. G., Yáñez, M. *J. Phys. Chem.* **90**, 5597-5604(1986).
- (27) Catalan, J., Palomar, J., de Paz, J. L. G. *Int. J. Mass. Spectrom. Ion Process* **175**, 51-59(1998).
- (28) Pulay, P. *Applications of Electronic Structure Theory*, H. F. Schaeffer III, ed.

- (1977), Plenum, New York, p. 153; Murtagh, B. A., Sargent, R. W. H. *Comput. J.* **131**, 185(1972); Schlegel, H. B. *J. Comput. Chem.* **3**, 214-218(1982).
- (29) Møller, C., Plesset, M. S. *Physical Review* **46**, 618-622(1934).
- (30) Fletcher, G. D., Rendell, A. P., Sherwood, P. *Molecular Physics* **91**, 431-438 (1997).
- (31) Roothaan, C. C. J., *Rev. Mod. Phys.* **23**, 69-89(1951).
- (32) Piecuch, P., Kucharski, S. A., Kowalski, K., Musial, M. *Comp. Phys. Commun.* **149**, 71-96(2002).
- (33) Kowalski, K., Piecuch, P. *J. Chem. Phys.* **113**, 18-35(2000).
- (34) Kowalski, K., Piecuch, P. *J. Chem. Phys.* **113**, 5644-5652(2000).
- (35) Krishnan, R., Binkley, J. S., Seeger, R., Pople, J. A. *J. Chem. Phys.* **72**, 650-654 (1980).
- (36) McLean, A. D., Chandler, G. S. *J. Chem. Phys.* **72**, 5639-(1980).
- (37) Garrett, B. C., Redmon, M. J., Steckler, R., Truhlar, D. G., Baldrige, K. K., Bartol, D., Schmidt, M. W., Gordon, M. S. *J. Phys. Chem.* **92**, 1476-1488(1988).
- (38) Schmidt, M. W., Gordon, M. S. *Annu. Rev. Phys. Chem.* **49**, 233-266(1998).
- (39) Edmiston, C., Ruedenberg, K. *Rev. Mod. Phys.* **35**(1963).
- (40) Curtiss, L. A., Raghavachari, K., Redfern, P. C., Pople, J. A. *J. Chem. Phys.* **106**, 1063-1079(1997).
- (41) Curtiss, L. A., Raghavachari, K., Trucks, G. W., Pople, J. A. *J. Chem. Phys.* **94**, 7221-7230(1991).
- (42) Schmidt, M. W., Baldrige, K. K., Boatz, J. A., Elbert, S. T., Gordon, M. S., Jensen, J. H., Koseki, S., Matsunaga, N., Nguyen, K. A., Su, S., Windus, T. L., Dupuis, M., Montgomery, J. A. *J. Comput. Chem.* **14**, 1347-1363(1993).
- (43) Schmidt, M. W., Gordon, M. S. *J. Mol. Struct. (THEOCHEM)*, in press.
- (44) *Gaussian 94*, Frisch, M. J., Trucks, G. W., Schlegel, H. B., Gill, P. M. W., Johnson, B. G., Robb, M. A., Cheeseman, J. R., Keith, T. A., Petersson, G. A., Montgomery, J. A., Raghavachari, K., Al-Laham, M. A., Zakrzewski, V. G., Ortiz, J. V., Foresman, J. B., Cioslowski, J., Stefanov, B., Nanayakkara, A., Challacombe, M., Peng, C. Y., Ayala, P. Y., Chen, W., Wong, M. W., Andres, J. L., Replogle, E. S., Gomperts, R., Martin, R. L., Fox, D. J., Binkley, J. S., Defrees, D. J., Baker, J., Stewart, J. P., Head-Gordon, M., Gonzalez, C., Pople, J. A.; Gaussian Incorporated, Pittsburgh PA 1995.
- (45) Bode, B. M., Gordon, M. S. *J. Mol. Graph. Model.* **16**, 133-138(1999).
- (46) Hehre, W. J., Ditchfield, R., Radom, L., Pople, J. A. *J. Am. Chem. Soc.* **92**, 4796-4801(1970).
- (47) Hammond, G. S. *J. Am. Chem. Soc.* **77**, 334-338(1955).

Table 1: Monosubstituted 1-H,3-R-1,3-pentazole (I) optimized geometries (bond lengths A-B in Å and angles A-B-C in degrees). For numbering system, see Figure 1.

	H	F	CH ₃	CN	NH ₂	OH	CH ₂ NO ₂	N ₃	NF ₂	C ₂ H ₃	OCH ₃
N3-R	1.026	1.299	1.476	1.372	1.355	1.322	1.459	1.361	1.463	1.433	1.310
N1- N2	1.313	1.318	1.314	1.314	1.322	1.320	1.313	1.320	1.312	1.315	1.321
N2- N3	1.313	1.311	1.317	1.325	1.321	1.315	1.317	1.325	1.313	1.323	1.323
N3- N4	1.328	1.321	1.334	1.348	1.339	1.331	1.334	1.347	1.332	1.342	1.337
N4- N5	1.313	1.319	1.312	1.310	1.314	1.317	1.312	1.314	1.314	1.310	1.320
N1- N5	1.328	1.327	1.326	1.328	1.320	1.323	1.327	1.322	1.332	1.326	1.320
N1- N2- N3	99.6	98.0	100.5	99.6	99.6	98.9	100.1	99.4	99.2	100.5	99.0
N2- N3- N4	115.1	117.4	113.7	114.4	114.5	115.7	114.1	114.4	115.7	113.4	115.2
N3- N4- N5	105.1	103.5	106.0	104.9	105.7	104.6	105.6	105.1	104.5	106.0	104.7
N4- N5- N1	105.1	105.6	105.0	105.7	105.5	105.3	105.1	105.4	105.4	105.2	105.4
N2- N1- N5	115.1	115.4	114.9	115.4	115.2	115.5	115.0	115.7	115.2	115.0	115.7
N2- N3-R	122.1	120.8	123.3	121.8	121.8	121.7	122.2	118.7	118.0	122.0	119.0
N4- N3-R	122.8	121.8	123.0	122.8	122.9	122.8	122.8	126.8	126.3	124.6	125.8

Table 2: Monosubstituted 1-H,2-R-1,2-pentazole (II) optimized geometries (bond lengths A-B in Å and angles A-B-C in degrees). For numbering system, see Figure 1.

	H	F	CH ₃	CN	NH ₂	OH	CH ₂ NO ₂	N ₃	NF ₂	C ₂ H ₃	OCH ₃
N2-R	1.027	1.304	1.479	1.369	1.379	1.325	1.474	1.363	1.464	1.434	1.313
N1- N2	1.311	1.311	1.315	1.320	1.318	1.312	1.315	1.319	1.311	1.320	1.318
N2- N3	1.321	1.309	1.325	1.344	1.330	1.317	1.330	1.334	1.325	1.332	1.322
N3- N4	1.327	1.336	1.328	1.322	1.324	1.338	1.326	1.334	1.327	1.326	1.342
N4- N5	1.327	1.329	1.324	1.328	1.335	1.321	1.326	1.320	1.334	1.325	1.318
N1- N5	1.321	1.327	1.324	1.320	1.314	1.330	1.322	1.329	1.319	1.323	1.331
N1- N2- N3	109.3	112.0	107.9	108.7	108.4	110.5	108.5	109.1	110.1	107.6	110.0
N2- N3- N4	105.2	103.4	106.2	104.8	105.5	104.4	105.6	105.0	104.4	106.1	104.5
N3- N4- N5	110.9	111.5	110.7	111.6	110.9	111.2	110.8	111.3	111.3	110.9	111.3
N4- N5- N1	105.2	105.5	105.0	105.4	105.0	105.5	105.3	105.5	105.2	105.0	105.6
N2- N1- N5	109.3	107.6	110.2	109.5	110.1	108.4	109.7	109.2	109.0	110.3	108.7
N1- N2-R	126.3	122.6	127.1	125.5	121.2	120.9	128.1	120.5	119.8	125.8	120.8
N3- N2-R	124.4	125.3	125.0	125.8	130.4	128.6	123.1	130.3	130.1	126.5	129.2

Table 3: MP2 and CR-CCSD(T)/6-311++G(d,p) electronic energy differences, in kcal/mol.

R=	H	F	CH ₃	CN	NH ₂	OH	CH ₂ NO ₂	N ₃	NF ₂	C ₂ H ₃	OCH ₃
1,3-											
isomer											
MP2	0.0	0.0	0.0	0.0	0.0	0.0	0.0	0.0	0.0	0.0	0.0
CR-	0.0	0.0	0.0	0.0	0.0	0.0	0.0	0.0	0.0	0.0	0.0
CCSD(T)											
1,2-											
isomer											
MP2	19.4	21.7	18.1	19.2	16.7	18.0	18.0	15.9	18.9	18.0	16.2
CR-	19.0	21.1	17.9	18.9	15.3	17.8	17.7	15.7	18.9	18.0	15.9
CCSD(T)											

Table 4: MCSCF/6-311++G(d,p) π orbital populations and bond orders.

π orbital populations						
	N1	N2	N3	N4	N5	Total bonding
1,3 ion	1.37	1.07	1.39	1.07	1.09	1.89
1,2 ion	1.42	1.42	1.04	1.06	1.04	1.89

adjacent π bond orders					
	N1-N2	N2-N3	N3-N4	N4-N5	N5-N1
1,3 ion	0.62	0.60	0.52	0.70	0.51
1,2 ion	0.49	0.58	0.62	0.62	0.58

next neighbor π bond orders					
	N1-N3	N2-N4	N3-N5	N4-N1	N5-N2
1,3 ion	-0.29	-0.22	-0.17	-0.15	-0.23
1,2 ion	-0.32	-0.16	-0.04	-0.16	-0.32

Table 5: Heats of formation at 298°K for gas-phase monosubstituted 1,3- and 1,2-pentazole cations. IA, IB, IIA, and IIB refer to particular resonance hybrids, with their average values being the predicted heats. The average is given in both kcal/mol and kcal/g.

R	1,3-isomer				1,2-isomer			
	$\Delta H_f^\circ(\text{IA})$	$\Delta H_f^\circ(\text{IB})$	average		$\Delta H_f^\circ(\text{IIA})$	$\Delta H_f^\circ(\text{IIB})$	average	
H	285.6	285.6	285.6	4.0	303.9	303.9	303.9	4.2
F	307.9	307.2	307.6	3.4	328.5	327.8	328.2	3.6
CH ₃	268.3	267.6	268.0	3.1	284.8	284.2	284.5	3.3
CN	358.1	358.5	358.3	3.7	376.6	377.0	376.8	3.9
NH ₂	302.2	301.0	301.6	3.5	318.3	317.1	317.7	3.7
OH	283.7	281.8	282.8	3.2	301.2	299.3	300.3	3.4
CH ₂ NO ₂	278.8	277.9	278.3	2.1	296.1	295.1	295.6	2.2
N ₃	393.6	391.0	392.3	3.5	409.2	406.6	407.9	3.6
NF ₂	317.3	313.9	315.6	2.6	335.4	332.1	333.7	2.7
C ₂ H ₃	294.6	293.3	294.0	3.0	311.1	309.8	310.5	3.2
OCH ₃	278.1	276.4	277.2	2.7	293.9	292.2	293.0	2.9

Table 6: Monosubstituted 1-H,3-R-1,3-pentazole transition state geometries (bond lengths A-B in Å and angles A-B-C in degrees). For numbering system, see Figure 1.

	H	F	CH ₃	CN	NH ₂	OH	CH ₂ NO ₂	N ₃	NF ₂	C ₂ H ₃	OCH ₃
N3-R	1.028	1.303	1.468	1.349	1.305	1.310	1.449	1.330	1.430	1.408	1.288
N1-	1.243	1.264	1.259	1.251	1.288	1.274	1.246	1.289	1.247	1.272	1.282
N2-											
N2-	1.243	1.267	1.238	1.253	1.275	1.267	1.249	1.270	1.259	1.246	1.272
N3-											
N3-	1.699	1.778	1.761	1.793	1.789	1.786	1.704	1.815	1.739	1.815	1.793
N4-											
N4-	1.181	1.181	1.182	1.180	1.193	1.186	1.182	1.191	1.184	1.183	1.189
N5-											
N1-	1.699	1.586	1.643	1.602	1.523	1.558	1.684	1.511	1.634	1.584	1.546
N5-											
N1-	115.8	112.0	116.3	114.7	111.4	112.2	115.7	111.7	113.7	115.5	111.8
N2-											
N2-	106.3	105.5	103.8	103.6	103.7	104.3	105.4	103.2	105.6	102.4	104.2
N3-											
N3-	105.7	100.9	104.4	102.6	101.2	101.4	106.2	100.4	103.6	102.3	101.1
N4-											
N4-	105.7	110.2	107.4	109.0	110.5	110.0	105.5	111.3	107.6	109.7	110.5
N5-											
N1-											
N2-	106.3	110.4	107.6	109.9	111.3	110.9	106.9	111.9	109.1	109.3	111.1
N1-											
N5-											
N2-	125.0	120.5	129.8	129.0	124.9	121.0	126.0	122.0	120.2	129.3	122.9
N3-R											
N4-	125.4	126.8	124.2	125.8	128.6	127.6	120.9	129.2	129.4	126.2	127.4
N3-R											

Table 7: Monosubstituted 1-H,2-R-1,2-pentazole ring-opened transition state geometries (bond lengths A-B in Å and angles A-B-C in degrees). For numbering system, see Figure 1.

	H	F	CH ₃	CN	NH ₂	OH	CH ₂ NO ₂	N ₃	NF ₂	C ₂ H ₃	OCH ₃
N2-R	1.029	1.330	1.470	1.347	1.353	1.345	1.460	1.364	1.461	1.402	1.327
N1- N2	1.285	1.318	1.275	1.301	1.310	1.316	1.288	1.313	1.303	1.284	1.319
N2- N3	2.012	1.836	2.065	1.985	2.013	1.929	2.033	1.969	1.956	2.029	1.948
N3- N4	1.152	1.171	1.149	1.156	1.156	1.163	1.152	1.160	1.157	1.153	1.162
N4- N5	1.368	1.390	1.355	1.373	1.365	1.377	1.375	1.365	1.387	1.352	1.369
N1- N5	1.318	1.309	1.330	1.318	1.320	1.313	1.315	1.319	1.307	1.332	1.317
N1- N2- N3	93.1	96.7	92.0	93.6	92.7	94.2	92.8	93.4	93.9	92.6	93.9
N2- N3- N4	89.6	95.0	88.0	90.9	89.9	92.6	89.1	91.4	91.9	89.2	91.8
N3- N4- N5	132.5	126.5	134.5	131.1	132.3	129.4	132.8	130.8	129.9	133.4	130.5
N4- N5- N1	101.3	101.9	101.0	101.9	101.6	101.7	101.4	101.7	101.5	101.3	101.6
N2- N1- N5	123.5	119.7	124.4	122.4	123.0	121.9	123.8	122.3	122.8	123.5	121.9
N1- N2-R	113.6	113.8	119.1	120.3	115.6	111.6	118.2	112.6	109.6	120.7	112.7
N3- N2-R	153.3	147.7	149.0	146.1	150.1	148.8	148.7	149.7	156.5	146.7	149.5

Table 8: Monosubstituted 1-H,2-R-1,2-pentazole geometries for the intermediates connecting the two transition states (bond lengths A-B in Å and angles A-B-C in degrees). For numbering system, see Figure 1.

	H	F	CH ₃	CN	NH ₂	OH	CH ₂ NO ₂	N ₃	NF ₂	C ₂ H ₃	OCH ₃
N2-R	1.029	1.345	1.460	1.353	1.299	1.334	1.462	1.344	1.466	1.389	1.315
N1-N2	1.265	1.287	1.254	1.290	1.270	1.275	1.269	1.279	1.281	1.268	1.280
N2-N3	3.295	3.353	3.306	3.305	3.297	3.346	3.302	3.323	3.338	3.306	3.328
N3-N4	1.135	1.137	1.136	1.137	1.139	1.138	1.137	1.139	1.136	1.137	1.139
N4-N5	1.307	1.305	1.299	1.309	1.281	1.293	1.305	1.288	1.312	1.294	1.289
N1-N5	1.329	1.329	1.342	1.320	1.377	1.346	1.329	1.351	1.318	1.345	1.353
N1-N2- N3	75.5	74.2	75.1	75.5	76.2	74.4	75.6	75.1	74.2	75.3	74.9
N2-N3- N4	38.0	37.6	38.7	38.3	40.3	38.3	38.4	39.1	37.6	39.3	39.1
N3-N4- N5	169.3	168.2	169.9	168.7	170.8	169.1	169.2	169.8	168.2	170.0	169.7
N4-N5- N1	109.7	110.7	109.6	110.4	110.3	110.9	110.3	110.8	110.3	110.1	110.7
N2-N1- N5	125.4	125.4	126.1	124.6	124.0	125.4	124.9	124.8	126.1	125.4	125.0
N1-N2-R	108.1	106.6	114.6	114.0	118.2	108.4	116.3	110.2	103.7	115.8	109.5
N3-N2-R	176.4	179.1	170.3	170.5	165.6	177.2	168.0	174.8	178.0	169.0	175.5

Table 9: Monosubstituted 1-H,2-R-1,2-pentazole geometries for the second transition state (bond lengths A-B in Å and angles A-B-C in degrees). For numbering system, see Figure 1.

	H	F	CH ₃	CN	NH ₂	OH	CH ₂ NO ₂	N ₃	NF ₂	C ₂ H ₃	OCH ₃
N2-R	1.029	1.359	1.482	1.356	1.303	1.374	1.439	1.220	1.490	1.422	1.296
N1- N2	1.255	1.308	1.240	1.270	1.249	1.312	1.291	1.294	1.272	1.248	1.273
N2- N3	3.925	4.123	3.945	3.957	2.291	3.844	3.469	4.078	4.151	3.973	4.326
N3- N4	1.122	1.122	1.122	1.122	1.144	1.120	1.130	1.140	1.122	1.122	1.140
N4- N5	1.961	2.113	1.939	2.000	1.392	2.583	1.524	1.290	2.095	1.965	1.289
N1- N5	1.217	1.214	1.227	1.213	1.400	1.217	1.253	1.402	1.206	1.226	1.378
N1- N2- N3	67.2	65.4	65.7	67.3	97.6	77.9	75.8	43.2	62.8	65.5	27.4
N2- N3- N4	33.8	25.0	34.2	33.4	43.9	33.5	33.6	34.3	32.8	34.4	10.4
N3- N4- N5	161.0	162.6	160.1	161.7	134.1	160.7	154.2	167.7	164.1	160.5	167.9
N4- N5- N1	102.1	102.6	102.1	102.1	110.0	81.1	109.0	108.8	102.7	102.1	109.5
N2- N1- N5	146.8	149.7	148.1	147.1	113.2	155.7	123.9	116.3	153.6	148.5	116.2
N1- N2-R	111.2	107.7	118.3	118.3	119.9	109.8	111.0	120.9	104.4	118.7	110.0
N3- N2-R	178.3	165.8	175.9	174.4	142.0	109.4	170.8	149.3	167.2	175.0	131.8

Table 10: Monosubstituted 1-H,3-R-1,3-pentazole decomposition product geometries (bond lengths A-B in Å and angles A-B-C in degrees). For numbering system, see Figure 1.

	H	F	CH ₃	CN	NH ₂	OH	CH ₂ NO ₂	N ₃	NF ₂	C ₂ H ₃	OCH ₃
N3-R	1.026	1.348	1.479	1.336	1.247	1.346	1.467	1.362	1.522	1.429	1.329
N1- N2	1.185	1.179	1.194	1.189	1.247	1.196	1.183	1.207	1.191	1.201	1.203
N2- N3	1.185	1.226	1.182	1.192	1.379	1.205	1.174	1.198	1.196	1.162	1.210
N3- N4	3.000	3.052	2.920	2.943	3.899	2.977	3.221	2.968	3.953	3.094	2.968
N4- N5	1.122	1.120	1.122	1.123	1.120	1.120	1.121	1.120	1.120	1.120	1.120
N1- N5	3.003	4.165	3.104	2.905	4.670	4.102	4.084	4.095	2.974	4.139	4.098
N1- N2- N3	156.9	163.2	157.6	154.2	114.5	160.3	165.1	157.0	155.3	165.7	157.8
N2- N3- N4	89.3	72.0	90.0	93.6	74.6	78.9	69.1	81.9	87.2	73.4	80.8
N3- N4- N5	101.2	158.9	105.7	94.2	170.9	162.5	169.5	170.2	18.9	166.0	166.9
N4- N5- N1	101.9	154.4	95.1	109.6	34.2	21.0	35.1	26.5	159.0	27.2	24.2
N2- N1- N5	88.8	75.5	87.4	88.0	86.6	81.8	80.0	83.6	77.5	78.3	83.0
N2- N3-R	129.6	111.1	136.3	136.1	113.1	115.3	127.1	119.2	123.3	134.1	116.4
N4- N3-R	134.9	78.7	129.2	129.2	38.5	109.9	73.9	96.4	147.4	83.1	100.0

Table 11: Monosubstituted 1-H,2-R-1,2-pentazole decomposition product geometries (bond lengths A-B in Å and angles A-B-C in degrees). For numbering system, see Figure 1.

	H	F	CH ₃	CN	NH ₂	OH	CH ₂ NO ₂	N ₃	NF ₂	C ₂ H ₃	OCH ₃
N2-R	1.025	1.358	1.480	1.336	1.247	1.346	1.389	1.132	1.523	1.425	1.329
N1- N2	1.184	1.235	1.181	1.190	1.376	1.206	1.268	1.323	1.196	1.183	1.210
N2- N3	4.071	5.719	4.107	3.961	3.916	4.066	4.252	4.071	3.965	4.078	4.051
N3- N4	1.120	1.120	1.120	1.120	1.120	1.120	1.120	1.139	1.120	1.120	1.120
N4- N5	3.000	2.797	3.047	2.946	4.792	3.071	3.158	1.296	2.967	3.044	3.102
N1- N5	1.184	1.168	1.193	1.188	1.246	1.195	1.145	1.431	1.191	1.197	1.203
N1- N2- N3	83.2	28.0	82.2	86.5	75.6	83.4	115.4	43.8	86.6	83.0	85.4
N2- N3- N4	16.1	15.4	13.3	18.6	7.9	12.8	17.5	23.4	18.4	12.7	13.2
N3- N4- N5	156.1	175.1	152.4	158.7	32.9	151.5	163.5	167.9	158.4	151.7	149.6
N4- N5- N1	77.8	122.4	76.4	78.3	83.5	74.8	73.9	106.8	77.8	76.0	75.0
N2- N1- N5	157.6	164.3	158.5	155.0	114.9	160.3	169.5	110.9	155.3	157.8	157.6
N1- N2-R	129.2	109.9	135.6	136.0	113.3	115.2	115.4	173.6	123.2	138.4	116.4
N3- N2-R	140.3	114.8	135.2	136.3	37.7	111.1	142.9	131.4	148.3	132.6	105.1

Table 12: Activation energies (E_a) for the decomposition of protonated pentazole to form the corresponding azidinium cations and N_2 (including zero-point energy correction, in kcal/mol). Subscripts 1 and 2 label the first and second activation energies, respectively, for the 1,2-isomer. E_{a2} is calculated relative to the global minimum energy structures shown in Figure 4.

R	1,3-isomer		1,2-isomer			
	E_a		E_{a1}		E_{a2}	
	MP2	CR- CCSD(T)	MP2	CR- CCSD(T)	MP2	CR- CCSD(T)
H	24.2	28.2	30.3	30.9	46.8	46.1
F	22.6	24.2	19.3	22.1	36.7	37.5
CH ₃	24.0	28.8	37.0	35.6	56.9	53.9
CN	19.0	22.4	19.0	22.3	37.3	39.3
NH ₂	18.7	22.6	30.5	24.6	50.5	57.8
OH	19.9	22.0	23.6	24.6	33.5	40.2
CH ₂ NO ₂	22.6	26.8	28.6	30.7	17.9	13.6
N ₃	16.0	20.2	23.4	25.2	14.1	6.4
NF ₂	19.7	23.3	21.0	23.4	34.2	39.3
C ₂ H ₃	21.8	26.8	32.0	31.1	42.4	50.8
OCH ₃	18.7	21.9	25.7	26.8	3.2	16.0

Table 13: Reaction energies, including zero point energy correction, for the decomposition of protonated pentazole to form the corresponding azidinium cations and N₂ (kcal/mol).

R	1,3-isomer		1,2-isomer	
	MP2	CR-CCSD(T)	MP2	CR-CCSD(T)
H	-18.3	-4.0	-38.3	-23.8
F	-18.2	-19.1	-43.3	-43.4
CH ₃	-16.7	-3.0	-35.1	-21.0
CN	-21.8	-7.1	-42.5	-26.5
NH ₂	-24.5	-31.1	-40.7	-46.4
OH	-20.1	-22.5	-37.0	-40.3
CH ₂ NO ₂	-22.8	-17.9	-56.1	-73.2
N ₃	-24.0	-25.2	-58.9	-56.3
NF ₂	-20.0	-3.5	-38.0	-22.1
C ₂ H ₃	-21.0	-17.9	-35.4	-21.8
OCH ₃	-19.9	-22.2	-35.0	-38.1

Table 14: Heats of proton transfer reaction, in kcal/mol, from the protonated pentazole to the anion = N(NO₂)₂⁻, NO₃⁻, and ClO₄⁻.

Anion=	N(NO ₂) ₂ ⁻	NO ₃ ⁻	ClO ₄ ⁻
1,3-isomer			
MP2	-131.3	-143.7	-121.0
CR-CCSD(T)	-126.9	-142.3	-117.9
1,2-isomer			
MP2	-150.7	-163.0	-140.3
CR-CCSD(T)	-145.8	-161.3	-136.9

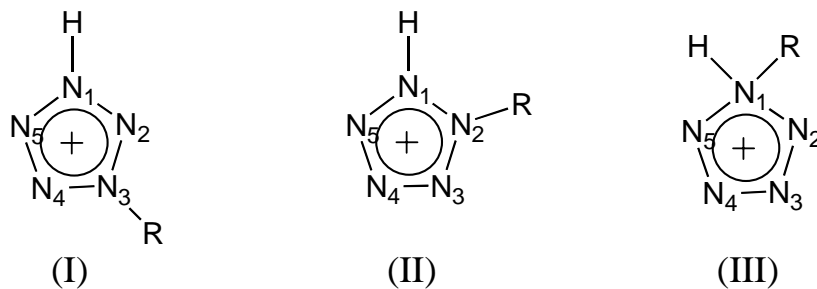
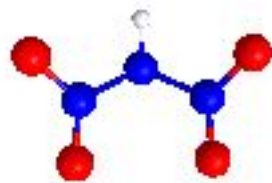
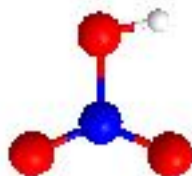


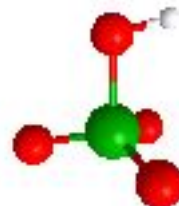
Figure 1: General structures of monosubstituted 1-H,3-R-1,3-pentazole (I), 1-H,2-R-1,2-pentazole (II), and 1-H,1-R-1,1-pentazole (III) cations showing the atom numbering around the ring.



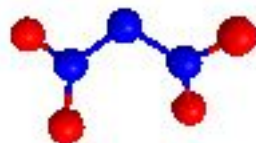
$\text{HN}(\text{NO}_2)$



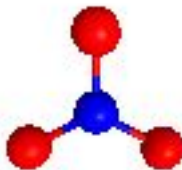
HNO_3



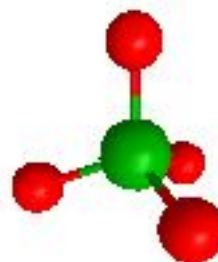
HClO_4



$\text{N}(\text{NO}_2)_2^-$



NO_3^-



ClO_4^-

Figure 2: Optimized structures of dinitramide, nitrate, and perchlorate anions (lower structures) and their protonated counterparts (nitrogen=blue, oxygen=red, chlorine=green, carbon=black, hydrogen=white).

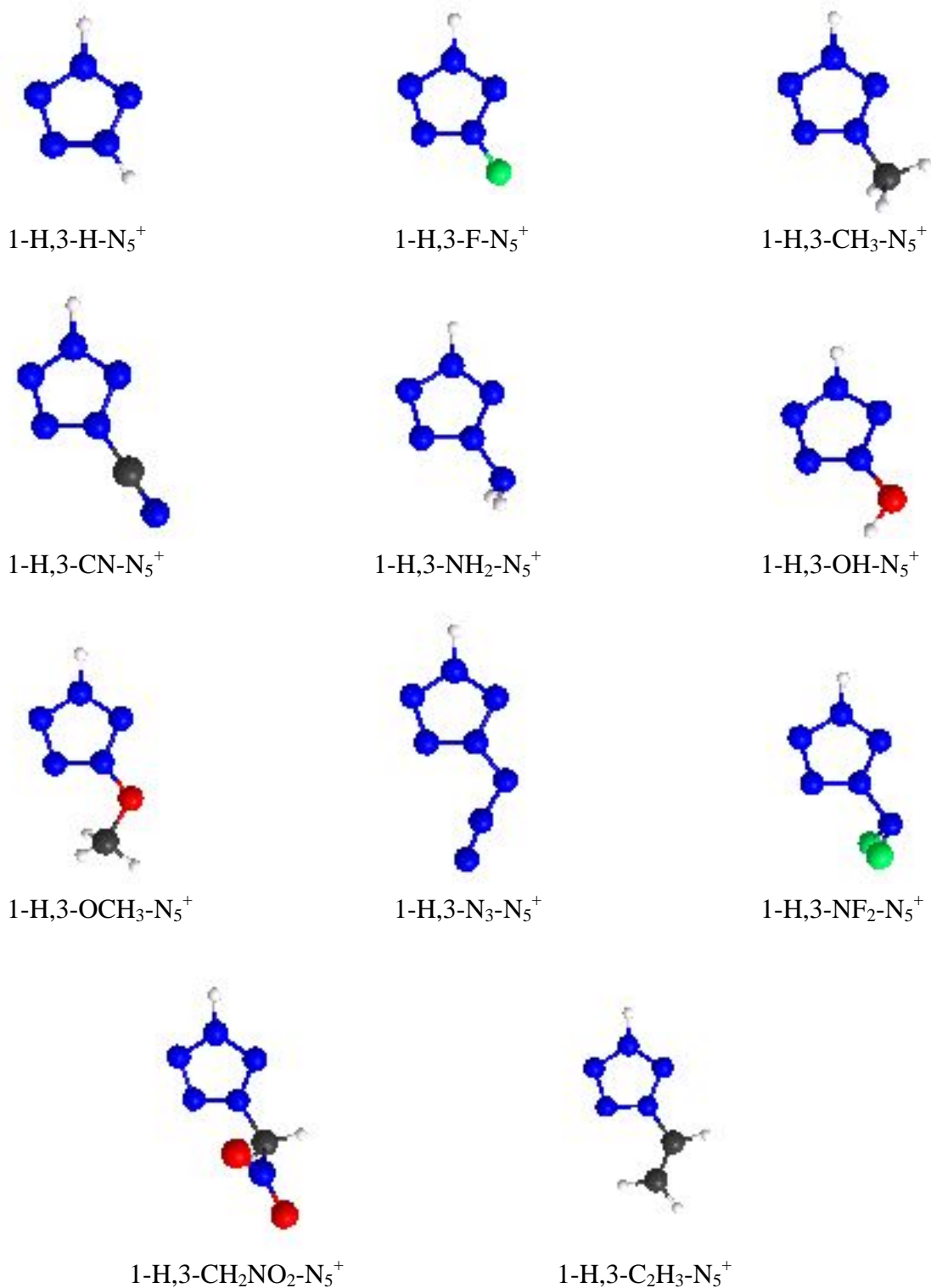
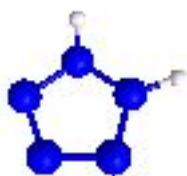
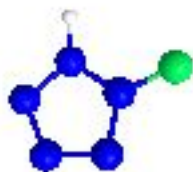


Figure 3: Monosubstituted 1-H,3-R-pentazole minimum energy structures (nitrogen=blue, oxygen=red, fluorine=green, carbon=black, hydrogen=white).



1-H,2-H-N₅⁺



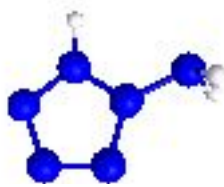
1-H,2-F-N₅⁺



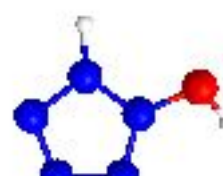
1-H,2-CH₃-N₅⁺



1-H,2-CN-N₅⁺



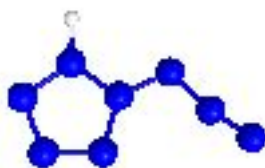
1-H,2-NH₂-N₅⁺



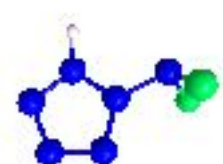
1-H,2-OH-N₅⁺



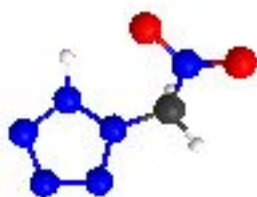
1-H,2-OCH₃-N₅⁺



1-H,2-N₃-N₅⁺



1-H,2-NF₂-N₅⁺



1-H,2-CH₂NO₂-
N₅⁺



1-H,2-C₂H₃-
N₅⁺

Figure 4: Monosubstituted 1-H,2-R-pentazole cation minimum energy structures. Atom colors as defined in Figure 3.

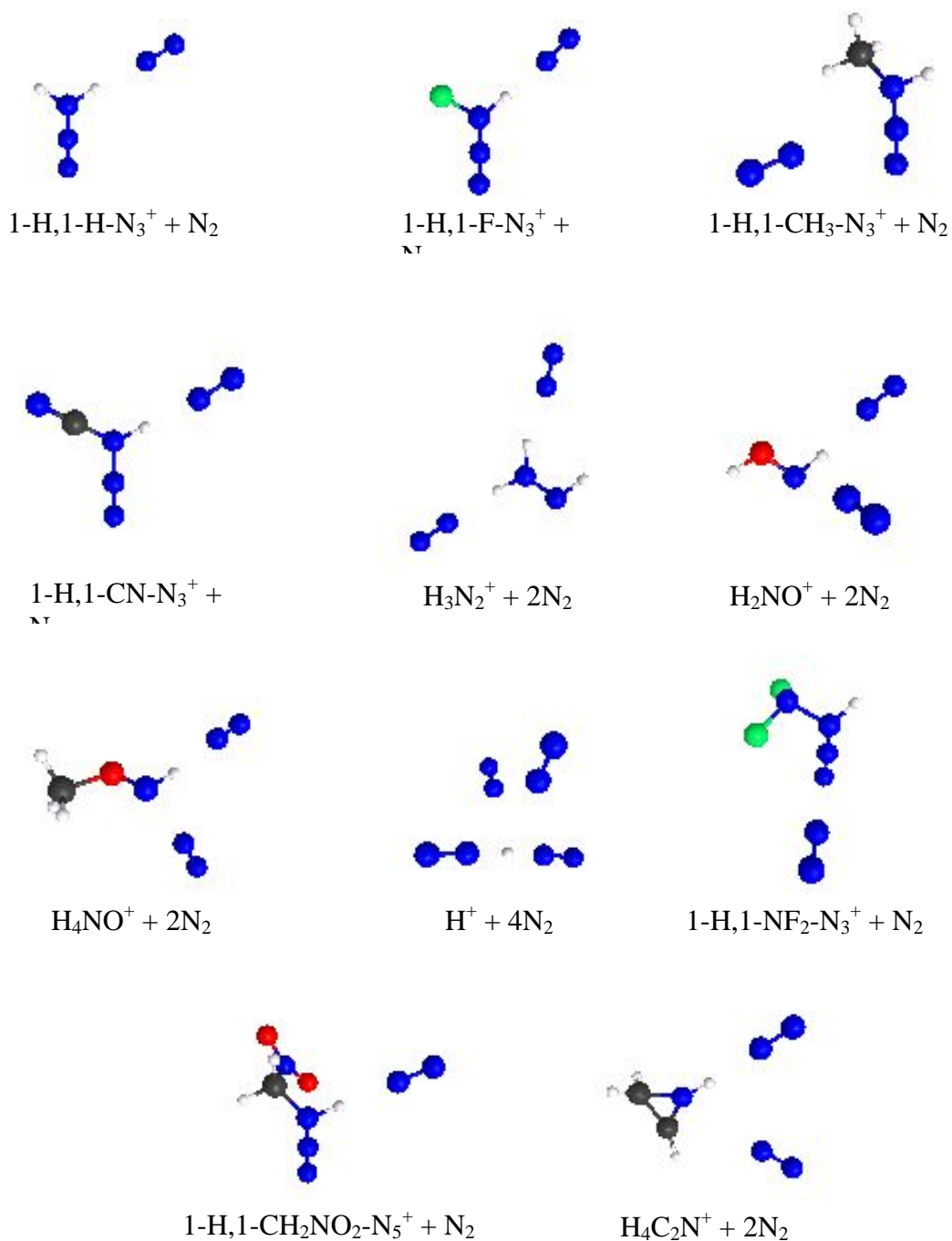


Figure 5: Isomer III minimum energy structures showing no stable ring species from the 1-H,1-R-pentazole cation. See last figure in Figure 1 for the starting structures. Atom colors as defined in Figure 3.

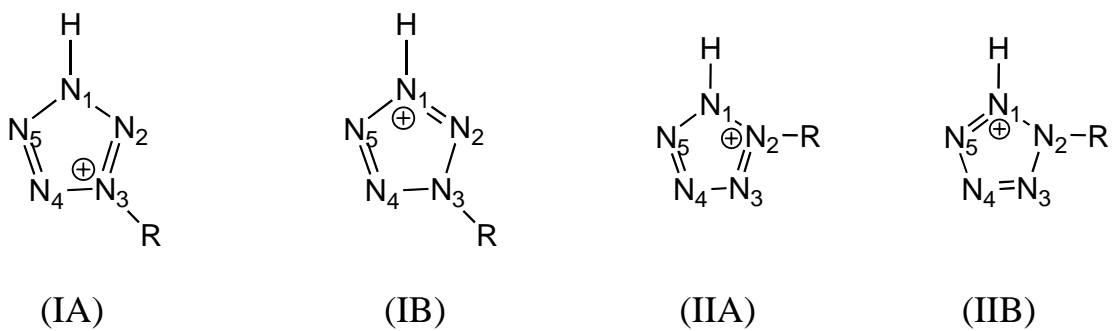


Figure 6: Contributing resonance structures for monosubstituted 1,3-pentazole (IA and IB) and 1,2-pentazole (IIA and IIB).

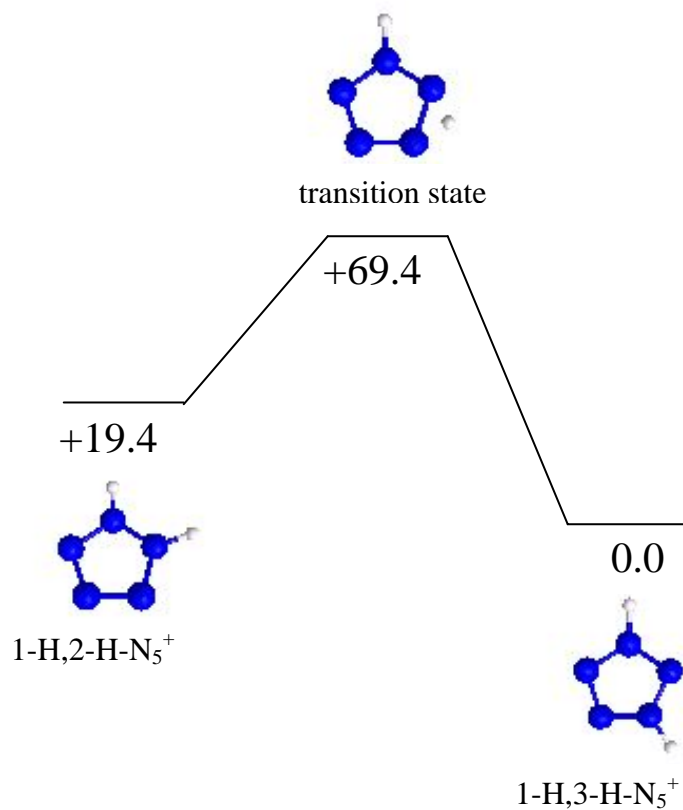


Figure 7: The MP2/6-311++G(d,p) relative energies in kcal/mol for proton rearrangement from the 1-H,2-H-pentazole to the 1-H,3-H-pentazole.

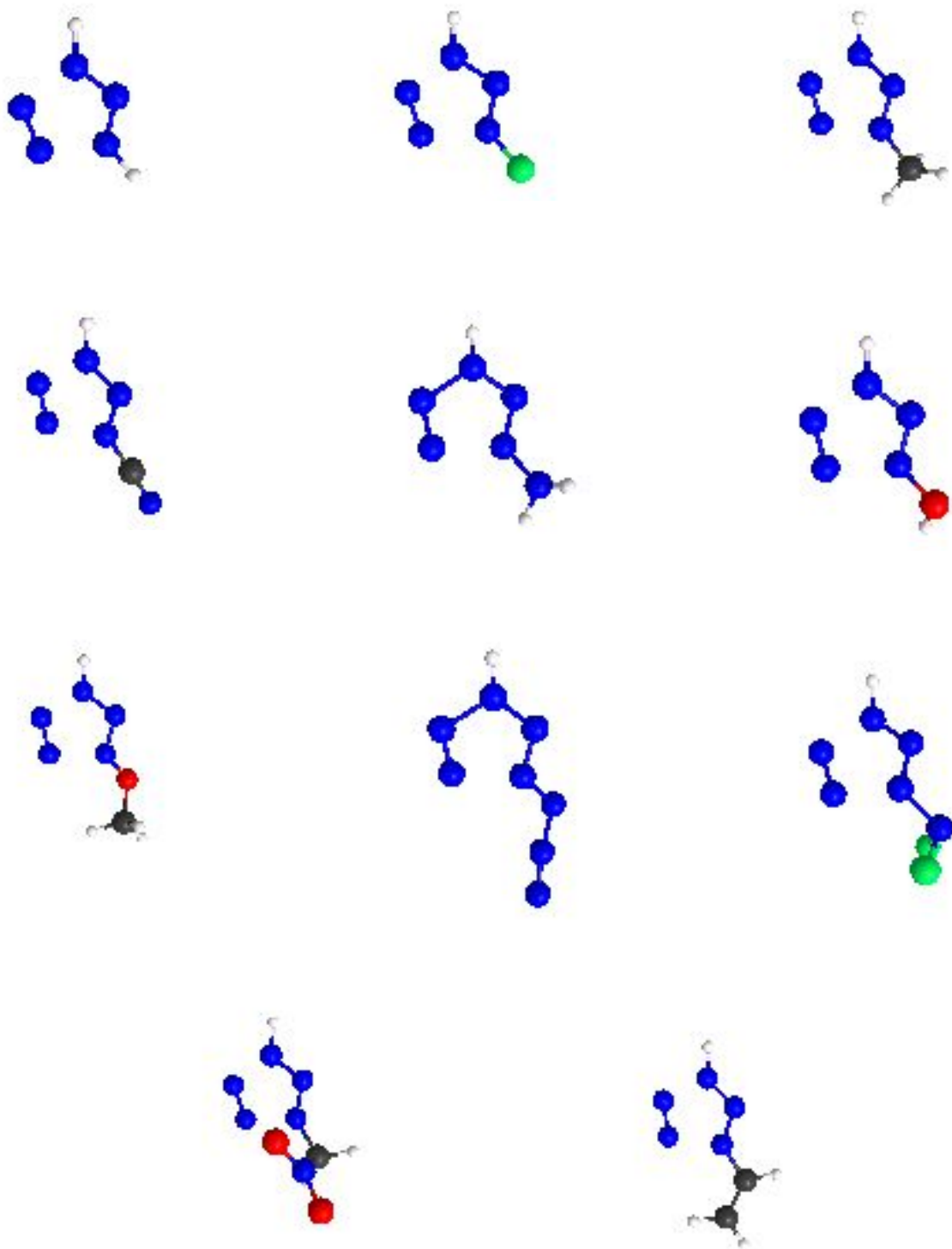


Figure 8: Monosubstituted 1-H,3-R-pentazole transition states. Atom colors as defined in Figure 3.

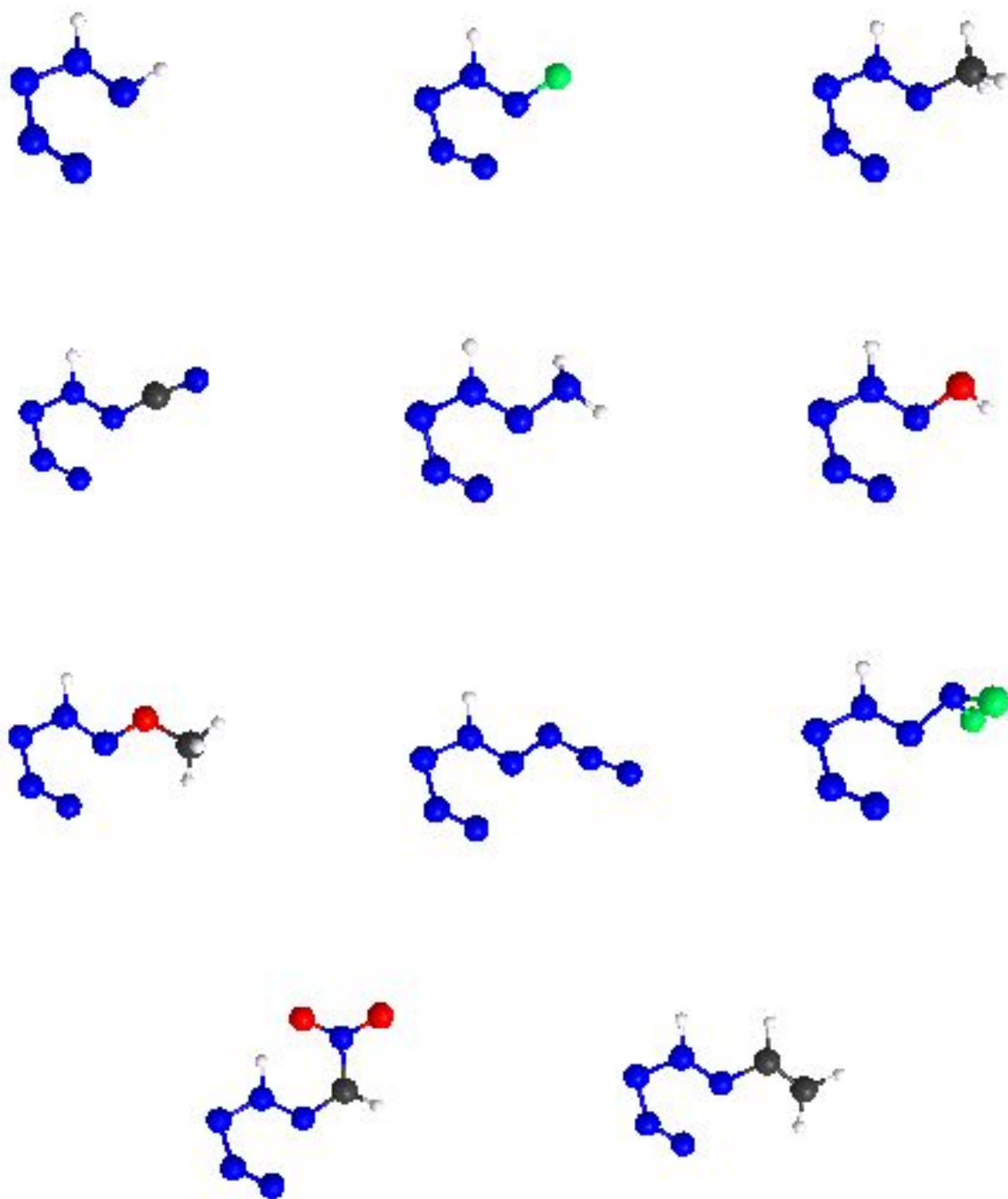


Figure 9: Monosubstituted 1-H,2-R-pentazole ring-opened transition states. Atom colors as defined in Figure 3.

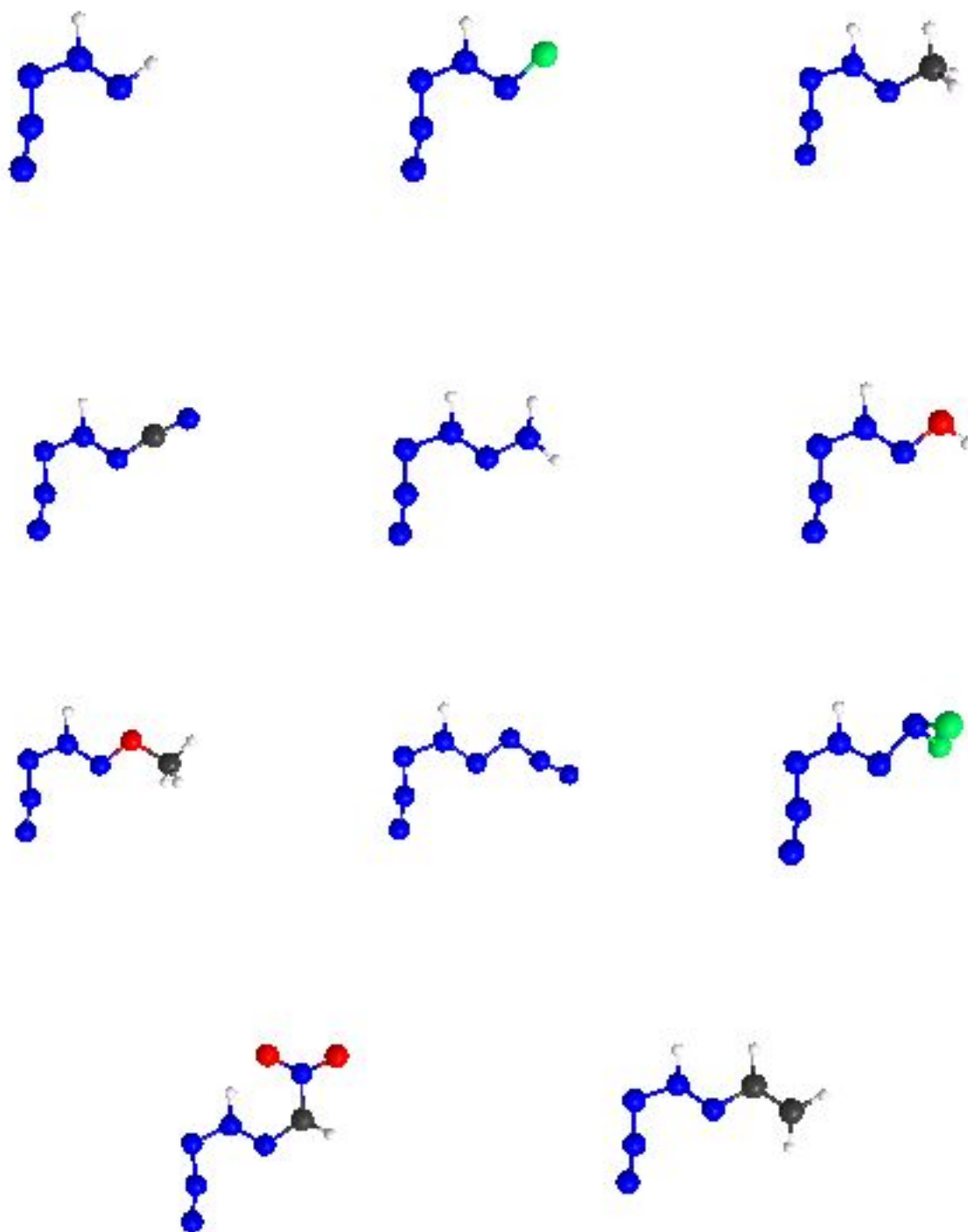


Figure 10: Local minima structures connecting the transition states of the monosubstituted 1-H,2-R-pentazole cations. Atom colors as defined in Figure 3.

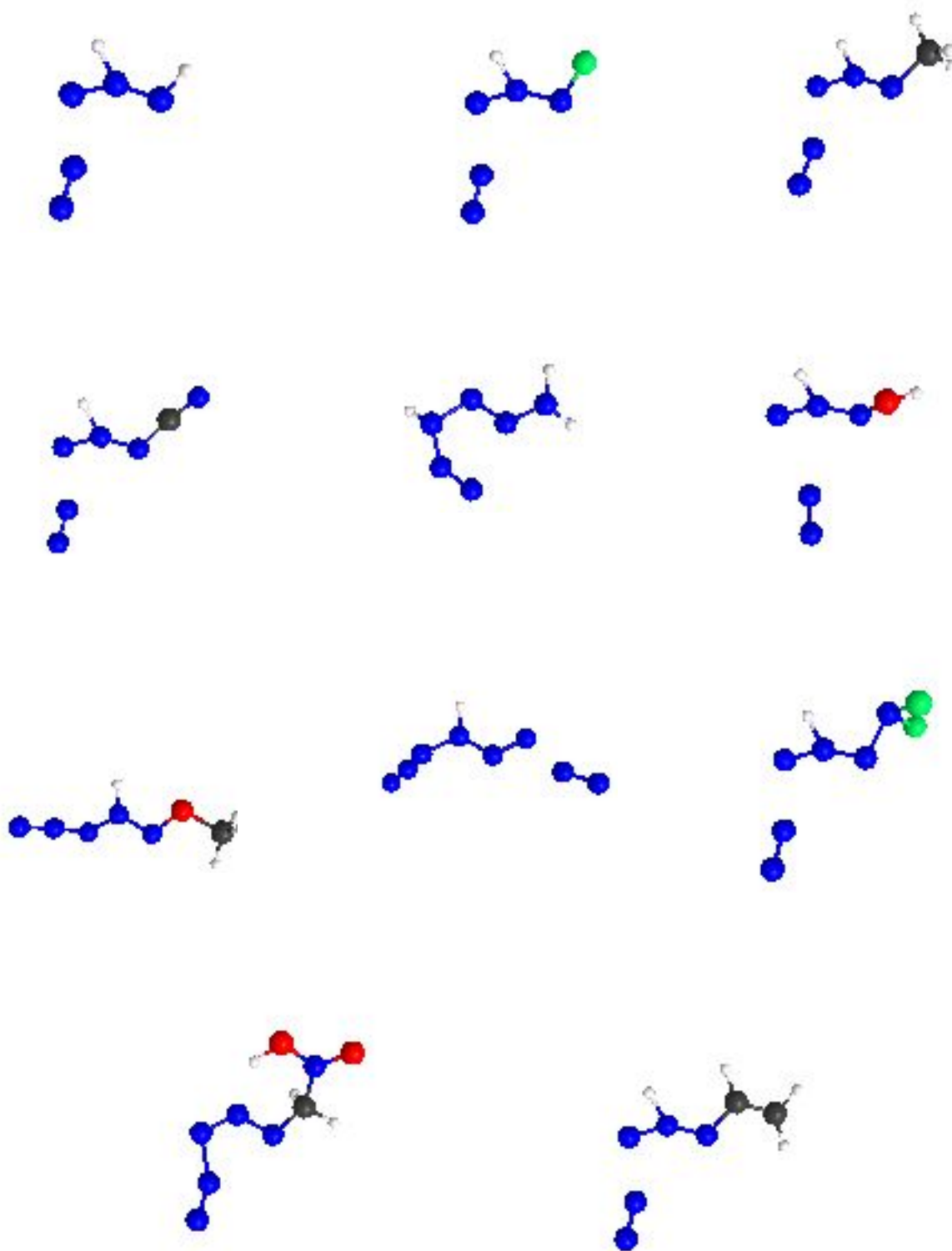


Figure 11: Monosubstituted 1-H,2-R-pentazole structures for the second transition state. Atom colors as defined in Figure 3.

This page is Distribution A: Approved for public release; distribution unlimited.

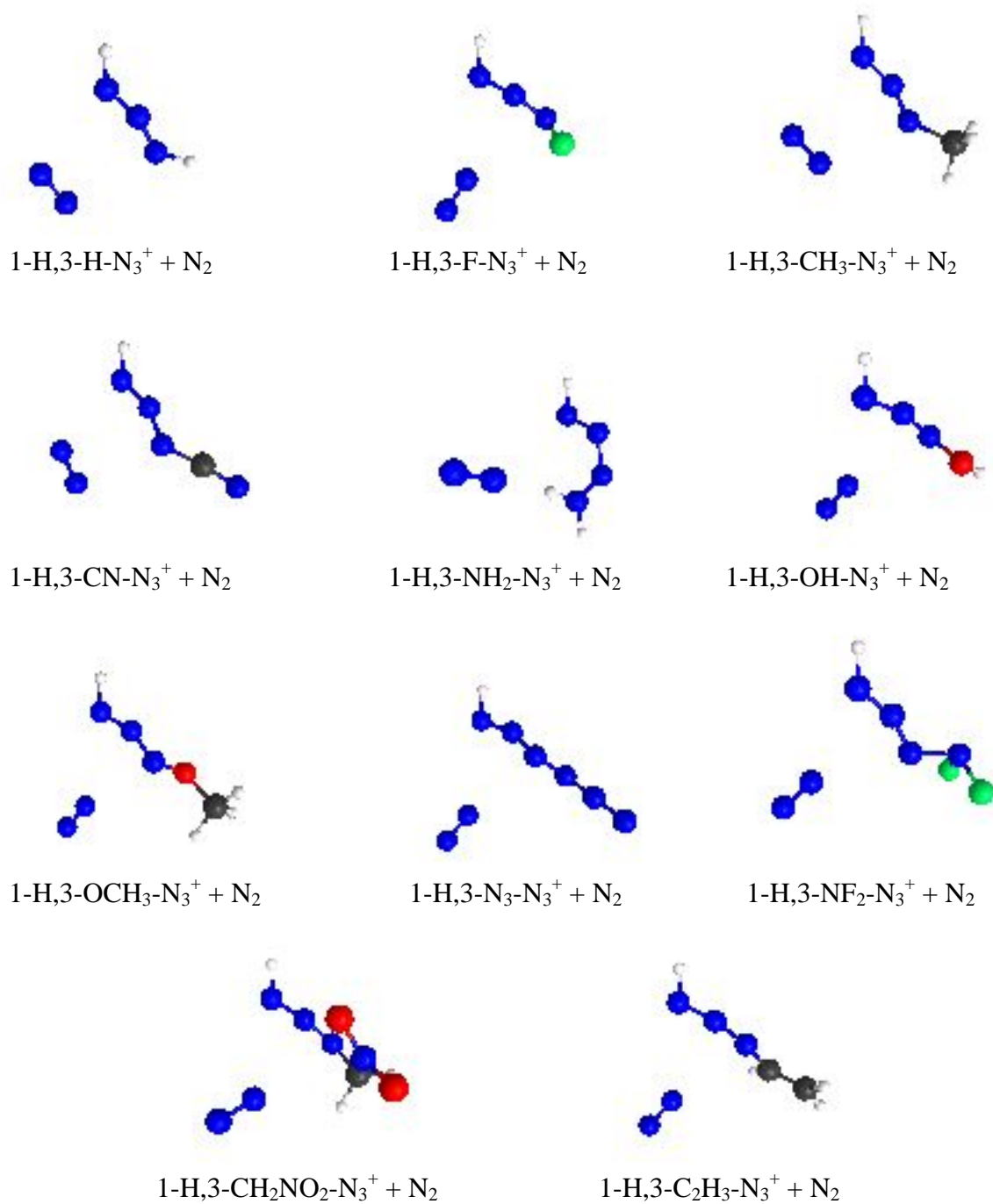


Figure 12: Monosubstituted 1-H,3-R-pentazole decomposition products. Atom colors as defined in Figure 3.

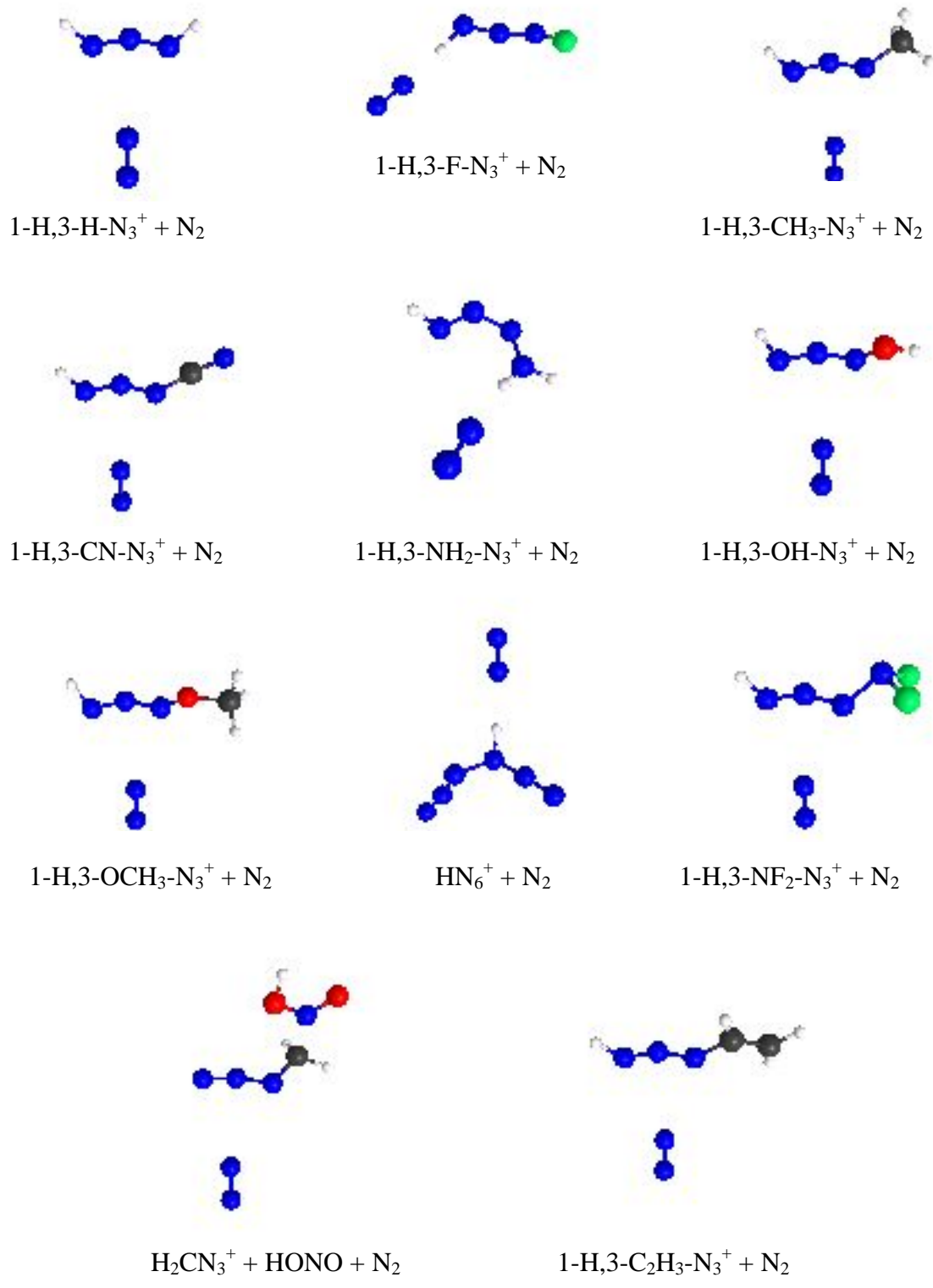


Figure 13: Monosubstituted 1-H,2-R-pentazole decomposition products. Atom colors as defined in Figure 3.

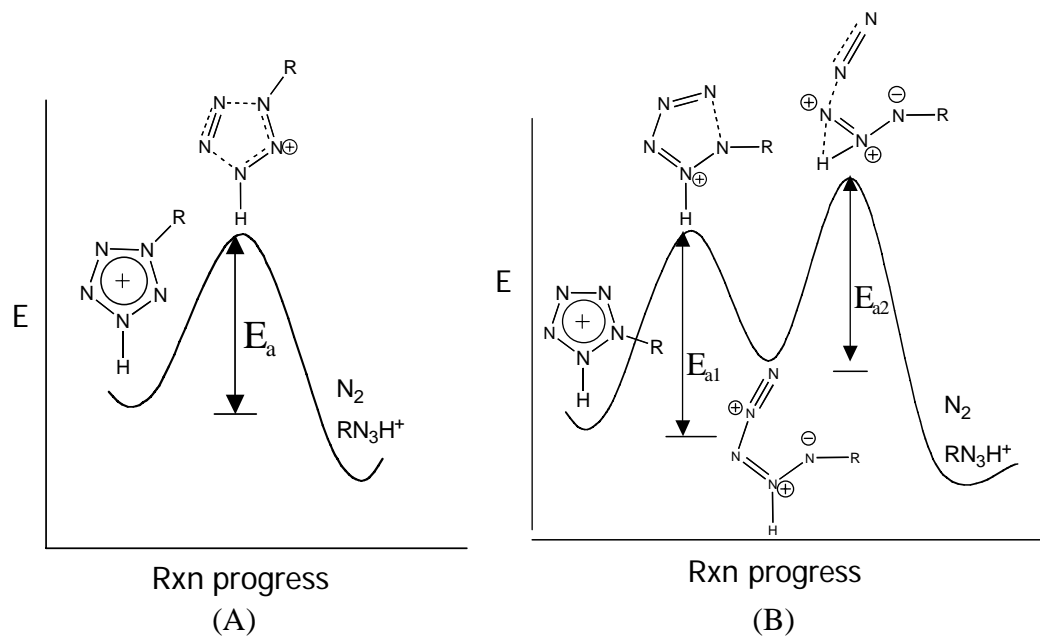


Figure 14: Decomposition pathways for the monosubstituted 1,3-isomer (A) and 1,2-isomer (B).

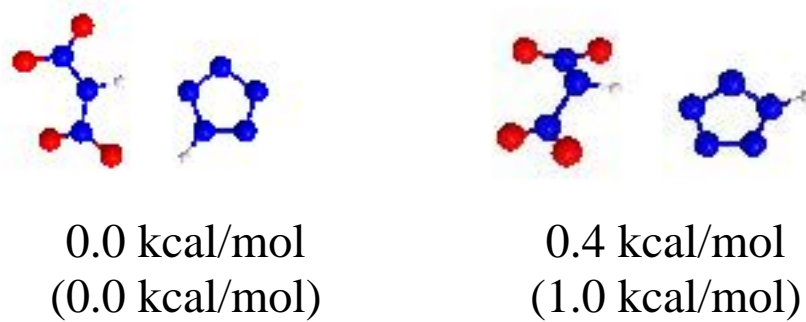


Figure 15: Minimum energy neutral dimer pairs formed by the protonated 1,2-pentazole (left) and 1,3-pentazole (right) with the dinitramide anion. Relative energies (beneath each structure) are from RHF/6-311++G(d,p). The MP2/6-311++G(d,p) relative energies at RHF geometries are in parenthesis. Atom colors as defined in Figure 3.

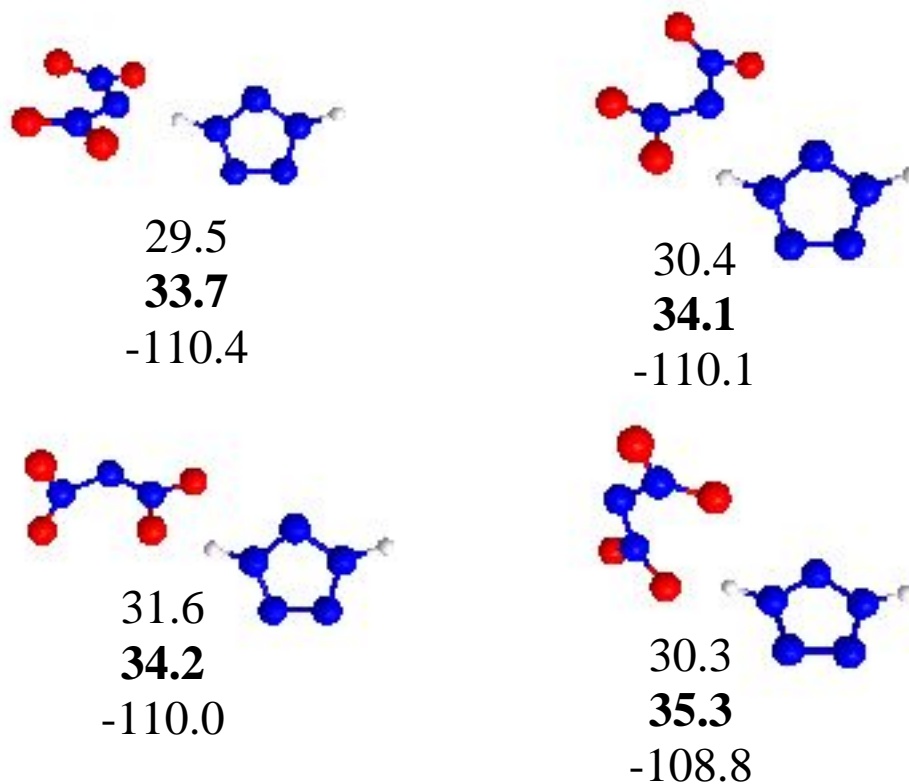


Figure 16: Ionic pairs in the parent 1,3-pentazole and dinitramide system, located at the RHF/6-311++G(d,p) level. The first and second energy values are from RHF/6-311++G(d,p) and MP2/6-311++G(d,p) at RHF geometries, in kcal/mol. The third energy value (if given) is the MP2 heat of reaction for $\text{HN}_5\text{H}^+ + \text{Y}^- \rightarrow [\text{HN}_5][\text{HY}]$ (or $[\text{HN}_5\text{H}^+][\text{Y}^-]$), where $\text{Y} = \text{N}(\text{NO}_2)_2, \text{NO}_3, \text{or ClO}_4$, in kcal/mol. The zero of energy for Figures 16-21 is a neutral complex presented in Figure 21. Atom colors as defined in Figure 3.

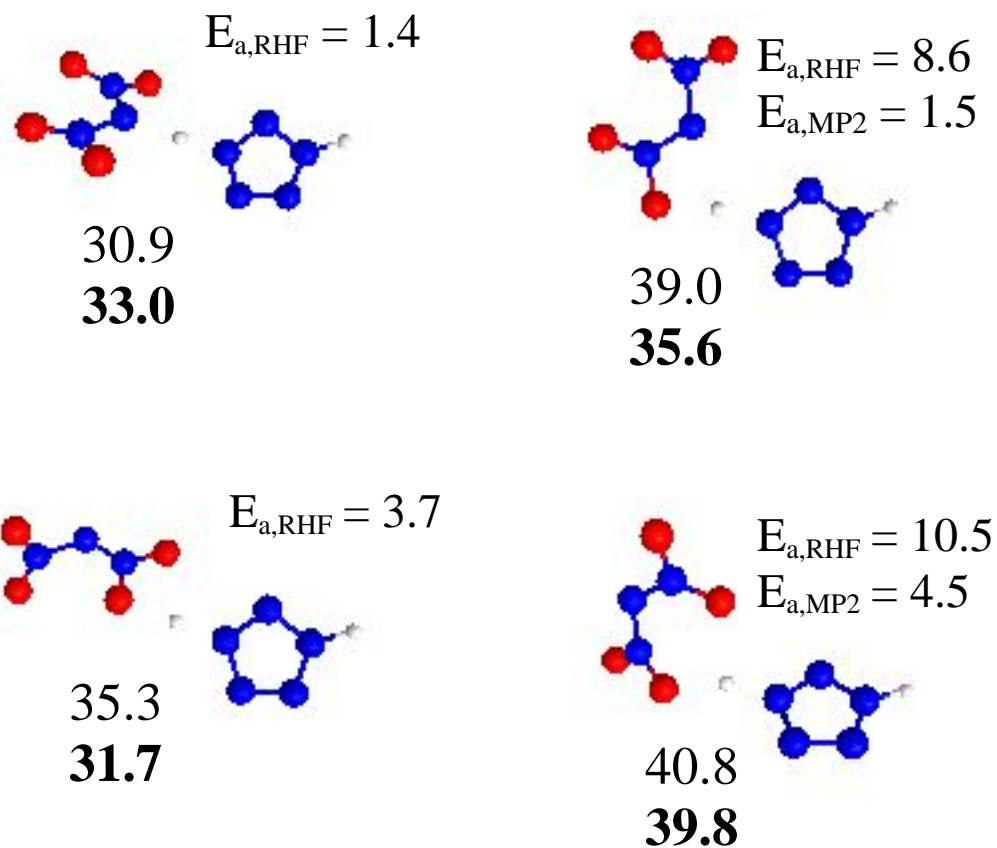


Figure 17: Transition states in the protonated 1,3-pentazole and dinitramide system, connecting ionic pairs to neutral complexes. The energy values and atom colors have the same meaning as defined in Figure 16. Activation energies (E_a) from RHF and MP2//RHF are calculated as the difference between the transition state and their corresponding ionic dimer energies, in kcal/mol.

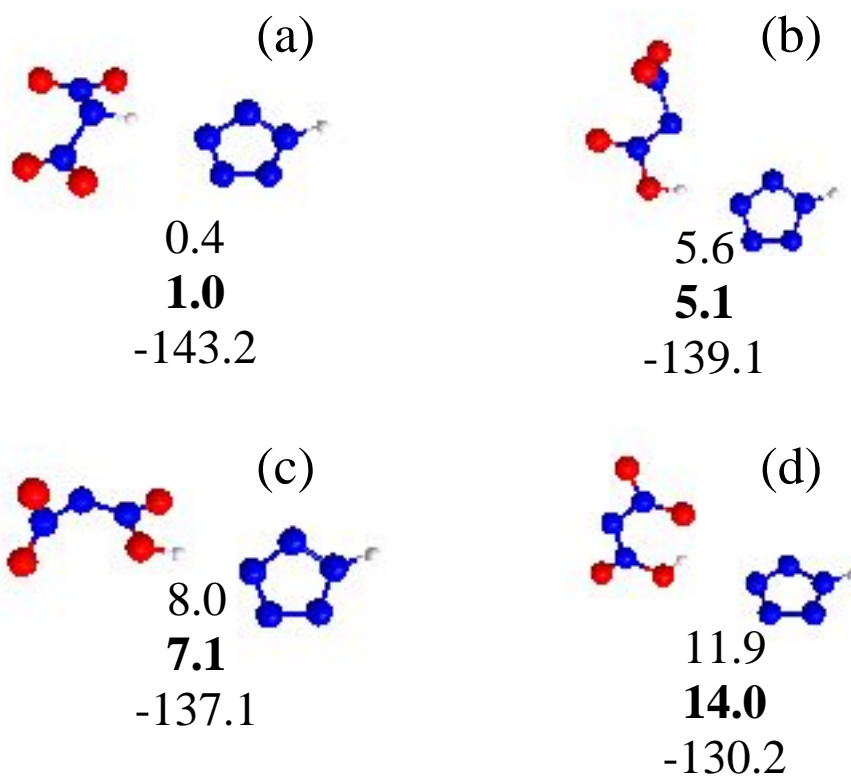


Figure 18: Neutral dimers in the protonated 1,3-pentazole and dinitramide system, resulting from proton transfers. The energy values and atom colors have the same meaning as defined in Figure 16.

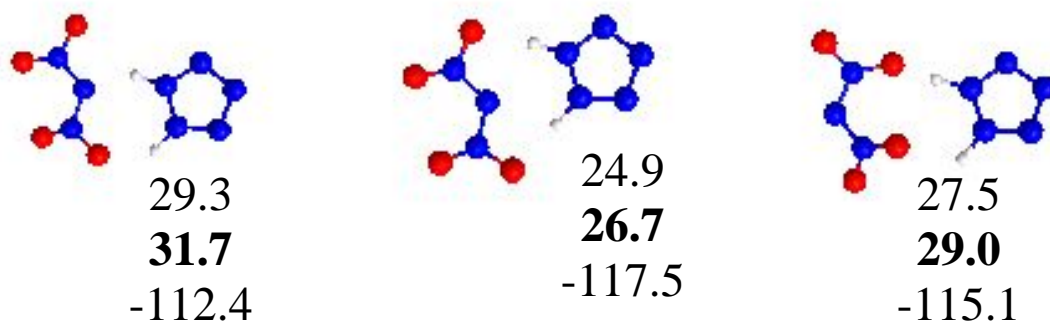


Figure 19: Ionic pairs in the parent 1,2-pentazole and dinitramide system. The energy values and atom colors have the same meaning as defined in Figure 16.

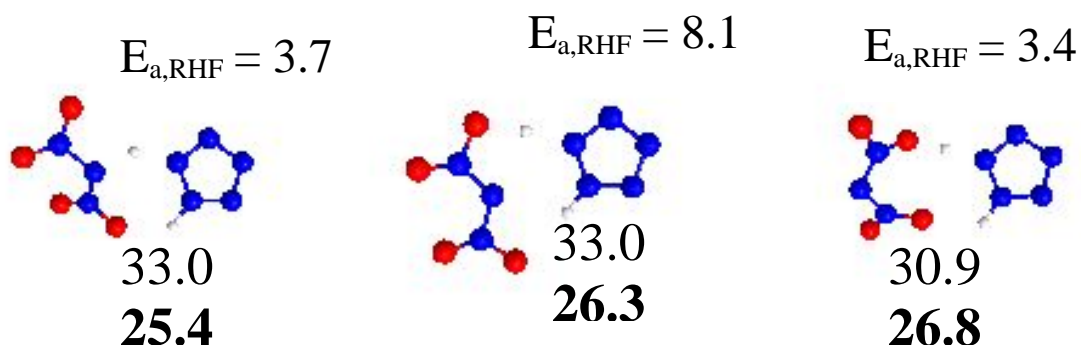


Figure 20: Transition states in the protonated 1,2-pentazole and dinitramide system, connecting ionic pairs to neutral complexes. The energy values and atom colors have the same meaning as defined in Figure 16. E_a values as defined in Figure 17.

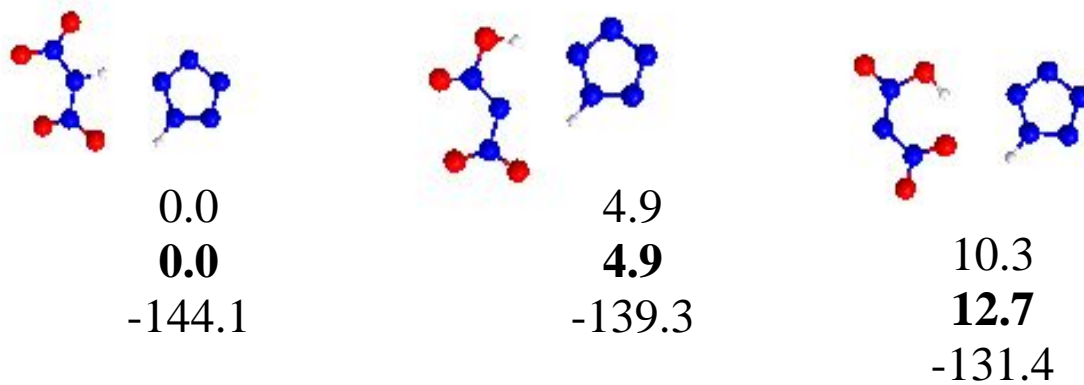


Figure 21: Neutral dimers in the parent 1,2-pentazole and dinitramide system, resulting from proton transfers. The energy values and atom colors have the same meaning as defined in Figure 16. The lowest energy dimer found is the leftmost structure, and is taken as the energy zero for Figures 16-21.

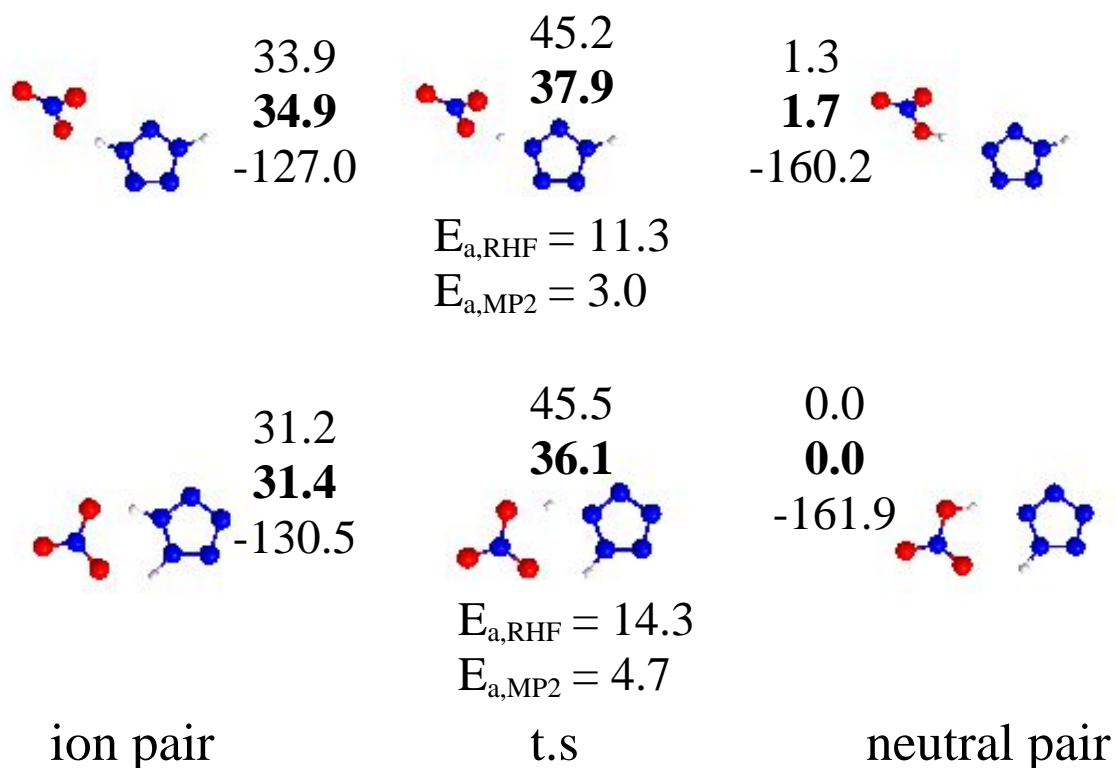


Figure 22: Structures for the parent 1,3-pentazole (upper) and 1,2-pentazole (lower) with nitrate: ion pair, transition state, and neutral pair. The energy values and atom colors have the same meaning as defined in Figure 16. E_a values as defined in Figure 17.

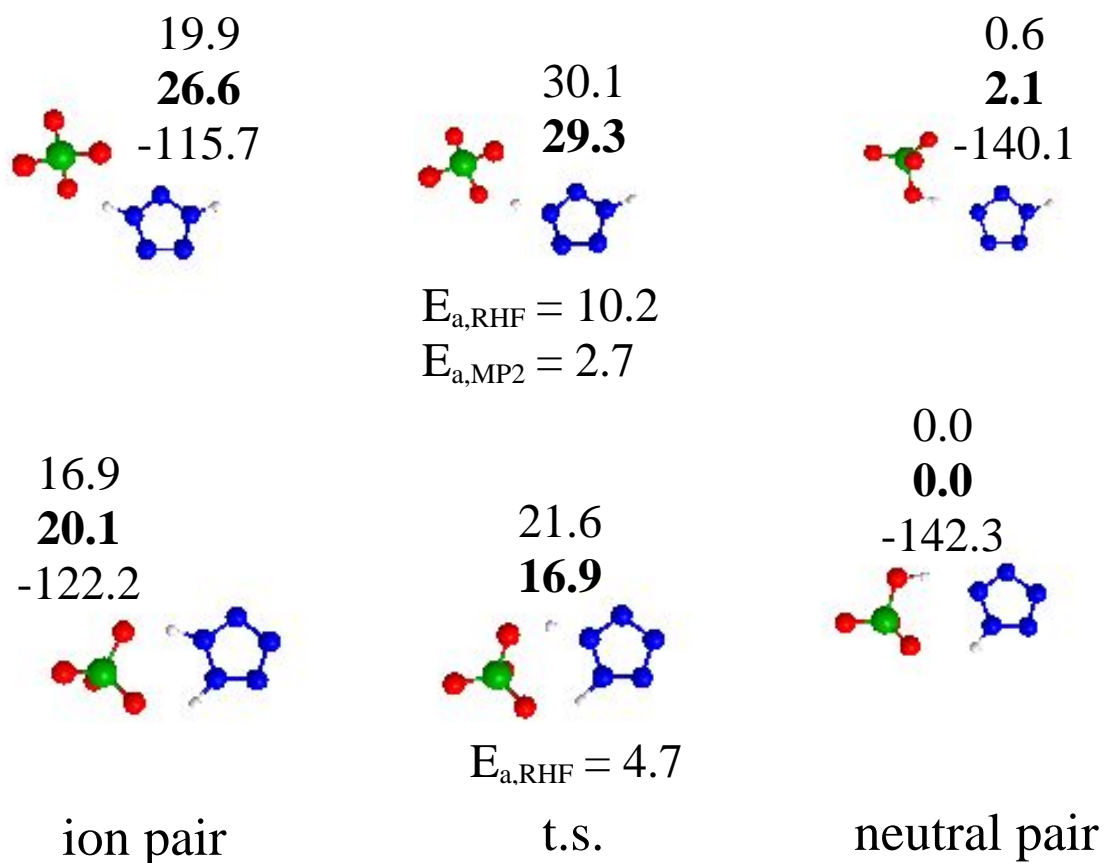


Figure 23: Structures for the parent 1,3-pentazole (upper) and 1,2-pentazole (lower) with perchlorate: ion pair, transition state, and neutral pair. The energy values have the same meaning as defined in Figure 16. Atom colors as defined in Figure 2. E_a values as defined in Figure 17.